PHYSICAL REVIEW D **80,** 075007 (2009)

LHC signals for warped electroweak charged gauge bosons

Kaustubh Agashe,[1] Shrihari Gopalakrishna,[2] Tao Han,[3] Gui-Yu Huang,[3,4] and Amarjit Soni[2]

[1]*Maryland Center for Fundamental Physics, Department of Physics, University of Maryland, College Park, Maryland 20742, USA*

[2]*Brookhaven National Laboratory, Upton, New York 11973, USA*

[3]*Department of Physics, University of Wisconsin, Madison, Wisconsin 53706, USA*

[4]*Department of Physics, University of California at Davis, Davis, California 95616, USA*

(Received 20 July 2009; published 7 October 2009)

We study signals at the LHC for the Kaluza-Klein (KK) excitations of electroweak *charged* gauge bosons in the framework of the standard model (SM) fields propagating in the bulk of a warped extra dimension. Such a scenario can solve both the Planck-weak and flavor hierarchy problems of the SM. There are two such charged states in this scenario with couplings to light quarks and leptons being suppressed relative to those in the SM, whereas the couplings to top/bottom quarks are enhanced, similar to the case of electroweak neutral gauge bosons previously studied. However, unlike the case of electroweak neutral gauge bosons, there is no irreducible QCD background (including pollution from possibly degenerate KK gluons) for decays to top + bottom final states so that this channel is useful for the discovery of the charged states. Moreover, decays of electroweak charged gauge bosons to longitudinal W, Z and Higgs are enhanced just as for the neutral bosons. However, unlike for the neutral gauge bosons, the purely leptonic (and hence clean) decay mode of the WZ is fully reconstructible so that the ratio of the signal to the SM (electroweak) background can potentially be enhanced by restricting to the resonance region more efficiently. We show that such final states can give sensitivity to 2(3) TeV masses with an integrated luminosity of 100(300) fb^{-1}. We emphasize that improvements in discriminating a QCD jet from a highly boosted hadronically decaying W, and a highly boosted top jet from a bottom jet will enhance the reach for these KK particles, and that the signals we study for the warped extra dimensional model might actually be applicable also to a wider class of nonsupersymmetric models of electroweak symmetry breaking.

DOI: 10.1103/PhysRevD.80.075007 PACS numbers: 12.60.Cn, 14.80.Cp

I. INTRODUCTION

The era of the LHC is upon us. Experiments at the LHC are highly expected to shed light on the mechanism of electroweak symmetry breaking (EWSB). In particular, various extensions of the standard model (SM) have been proposed to solve the problem in the SM of the hierarchy between the Planck and electroweak scales. Such models predict the existence of new particles at the weak (or TeV) scale which are likely to be accessible to the LHC.

In the present work, we focus on one such extension of the SM, the Randall-Sundrum model (RS1) [1] with all the SM fields propagating in the bulk of a warped extra dimension [2–4]. Such a framework can address the flavor hierarchy problem of the SM as well. The versions of this framework with a grand unified gauge symmetry in the bulk can naturally lead to precision unification of the three SM gauge couplings [5] and a candidate for the dark matter of the universe (the latter from requiring longevity of the proton) [6]. The new particles in this framework are Kaluza-Klein (KK) excitations of all SM fields with masses at ~TeV scale. So far, studies of the LHC signals from direct production of the radion [7], KK gluon [8–11], graviton [12], *neutral* electroweak gauge bosons [13], (heavy) fermions [14], and finally *light* KK fermions present in some models with extended 5D gauge symmetries [15] in such a framework have been performed (see Ref. [14] for an overview and Refs. [16] for related studies in other setups within the warped extra dimensional framework).

However, there are some challenging aspects of this collider phenomenology as follows. First, the KK mass scale is constrained to be at least a few TeV by the electroweak and flavor precision tests, in part due to the absence of a parity symmetry [analogous to R parity in supersymmetry (SUSY)], allowing tree-level exchanges to contribute to the precision observables. In addition, the constituents of the proton (or SM gauge bosons and light fermions, in general) couple weakly to the KK states, whereas the KK states mostly decay to top quarks and longitudinal W/Z/Higgs due to a larger coupling to these states. As a result, the golden decay channels such as resonant signals of dileptons or diphotons are suppressed. Finally, given the few TeV KK mass, the top quarks/W/Z resulting from the decays of these KK states are highly boosted, creating problems in their identification due to collimation of their decay products.

In light of this situation, it is necessary to study as many LHC probes of this framework as possible, especially since there might not be a single ''smoking gun'' for this framework; i.e., a variety of channels can complement each other as far as detecting this framework at the LHC is concerned.

In particular, the most widely studied particle is the KK gluon, which decays only to jetty final states, but has the largest cross section due to the QCD coupling (assuming the same mass for all KK particles as in the simplest models). It was found that the LHC reach can be $\sim$4 TeV, using techniques designed specifically to identify highly boosted top quarks. However, it is good to have channels with no jets if possible since, in general, such modes are cleaner in the LHC experimental environment.

Also, it is obviously important to explore the feasibility of searching for the electroweak (EW) KK states (i.e., excitations of γ, W, and Z) at the LHC. In fact, decays of EW KK states to (longitudinal) W/Z and Higgs offer a possibility for clean final states if these SM particles decay to leptons (note that the direct decays to leptons/photons are suppressed, as mentioned above). However, the decay of the KK Z to WW followed by leptonic decays of both W's has two neutrinos in the final state so that the invariant mass of the W pair cannot be effectively reconstructed, making it harder to identify the signal and to reduce the continuum SM WW background. If one W decays instead to a pair of quarks (we call it ''semileptonic'' decay of the WW gauge-boson pair), then the problem is that the two jets from the W are collimated, introducing a larger QCD background from W + jet. A similar analysis applies to decays of the KK Z to the Zh final state. Finally, one could utilize decays to top pairs for detecting the KK Z using techniques to identify boosted tops developed for detecting the KK gluon, but this channel is swamped by decays of the KK gluon to (i.e., resonant production of) top pairs, if not by the SM $t\bar{t}$ continuum background.

Given this situation, the KK W can provide (*a priori*) a couple of advantages:

(i) The decays to WZ followed by (clean) leptonic decays of both W and Z can be more effectively reconstructed due to the presence of only one neutrino.

The semileptonic decays of WZ or Wh face similar challenges to those of KK Z, namely, QCD Z/W + jet background, and we can use a jet-mass cut in order to reduce this background, i.e., to distinguish a W/Z jet from a QCD jet.

(ii) The decays of KK W to $t\bar{b}$ do not have the contamination from the KK gluon as in the case of KK Z.

With this background, we are thus motivated to study signals for the KK excitation of the SM W in this paper. With detailed parton-level simulations for the signal and SM backgrounds, we find the reach for this particle to be 2(3) TeV with $\sim$100(300) fb^{-1} luminosity in the best of the $t\bar{b}$, WZ, and Wh channels, a discovery potential which is roughly similar to that for the KK Z, found earlier in [13]. The reason for the similar (although slightly better) reach for the KK W as for the KK Z, in spite of the above two advantages expected for the former, are that, first, the branching ratios (BR) to leptons for the SM Z is smaller than that for the W, making the final significance of the leptonic decays of the WZ from the KK W not much better than in the case of the purely leptonic decays of the W pairs from the KK Z. Second, we find that a highly boosted top quark can fake a bottom quark so that QCD or KK-gluon $t\bar{t}$ pairs do manifest as *reducible* backgrounds to the $t\bar{b}$ signal from the KK W. Once again, we use a jet-mass cut, this time to discriminate between a t jet and a b jet. Anticipating more dedicated analyses in regard to vetoing $t\bar{t}$ background from KK-gluon decays, we believe that it is possible to improve the reach for KK W in the $t\bar{b}$ channel. Similarly, further improvements in the jet-mass technique of distinguishing a W/Z jet from a QCD jet or the development of new ones to reduce this QCD background can increase the reach for *both* KK W and Z in semileptonic WW/WZ decays of these KK modes. We observe that for the W', all SM decay modes could be useful, whereas for the Z', as discussed above, the $t\bar{t}$ channel with a significant BR is not. Therefore, combining all SM channels, we expect the reach in W' to be better than the Z'.

The outline of the paper is as follows. In Sec. II, we begin with a brief review of the theory of a warped extra dimension and the LHC signals for the KK states, including an outline of the various cases we consider for the study of the electroweak charged gauge bosons. We present the total decay widths of W''s and the branching ratios to various channels in Sec. III. In Sec. IV, we calculate the production cross sections of the charged gauge bosons at the LHC and present a detailed analysis of how to obtain signals for these states. The framework of warped extra dimensions is conjectured to be dual to four-dimensional (4D) strong dynamics triggering electroweak symmetry breaking, as in technicolor or composite Higgs models. In Sec. V, we then compare the signals that we studied in a warped extra dimension to the signals for technicolor models discussed previously (since the 1990s). Further discussions and conclusions are presented in Sec. VI, where we argue that many of the signals that we study here (including the electroweak neutral gauge-boson case studied earlier) might be applicable to a wider class of nonsupersymmetric models of EWSB. Finally, two appendixes are included at the end to provide further details for the model, including the couplings of the W' states.

II. REVIEW OF WARPED EXTRA DIMENSION

The framework consists of a slice of anti–de Sitter (AdS) space in five dimensions (AdS_5), where (due to the warped geometry) the effective 4D mass scale is dependent on the position in the extra dimension. The 4D graviton, i.e., the zero mode of the 5D graviton, is automatically localized at one end of the extra dimension (called the Planck/UV brane). If the Higgs sector is localized at the other end [in fact, with the SM Higgs originating as the fifth compo-

nent of a 5D gauge field (A_5), it is automatically so [17]], then the warped geometry naturally generates the Planck-weak hierarchy. Specifically, TeV $\sim \bar{M}_P e^{-k\pi r_c}$, where $\bar{M}_P$ is the reduced 4D Planck scale, k is the AdS_5 curvature scale, and r_c is the proper size of the extra dimension. The crucial point is that the required modest size of the radius (in units of the curvature radius), i.e., $kr_c \sim 1/\pi \log(\bar{M}_P/\mathrm{TeV}) \sim 10$, can be stabilized with only a corresponding modest tuning in the fundamental or 5D parameters of the theory [18]. Remarkably, the correspondence between AdS_5 and 4D conformal field theories (CFT) [19] suggests that the scenario with warped extra dimensions is dual to the idea of a composite Higgs in 4D [17,20].

It was realized that with SM fermions propagating in the bulk, we can also account for the hierarchy between quark and lepton masses and mixing angles (flavor hierarchy) as follows [3,4]: the basic idea is that the 4D Yukawa couplings are given by the product of the 5D Yukawa couplings and the overlap of the profiles in the extra dimension of the SM fermions (which are the zero modes of the 5D fermions) with that of the Higgs. The light SM fermions can be localized near the Planck brane, resulting in a small overlap with the TeV-brane-localized SM Higgs, while the top quark is localized near the TeV brane with a large overlap with the Higgs. The crucial point is that such vastly different profiles can be realized with small variations in the 5D mass parameters of fermions. Thus we can obtain hierarchical SM Yukawa couplings without any large hierarchies in the parameters of the 5D theory, i.e. the 5D Yukawas and the 5D masses. Because of the different profiles of the SM fermions in the extra dimension, flavor changing neutral currents (FCNC) are generated by their nonuniversal couplings to gauge KK states. However, these contributions to the FCNC are suppressed due to an analog of the Glashow-Iliopoulos-Maiani (GIM) mechanism of the SM, i.e. RS-GIM, which is ''built in'' [4,21,22]. The point is that *all* KK modes (whether gauge, graviton, or fermion) are localized near the TeV or IR brane (just like the Higgs) so that nonuniversalities in their couplings to SM fermions are of the same size as couplings to the Higgs.

In spite of this RS-GIM suppression, it was shown recently [23] (see also [24,25]) that the constraint on the KK mass scale from contributions of the KK gluon to ϵ_K is quite stringent. In particular, for the model with the SM Higgs (strictly) localized on the TeV brane, the limit on the KK mass scale from ϵ_K is $\sim$10–40 TeV, depending on the size of the 5D QCD gauge coupling. However, the phenomenology of the TeV-scale KK modes and the SM Higgs is quite sensitive to the structure near the TeV brane (where these particles are localized). For example, the SM Higgs can be the lightest mode of a 5D scalar (instead of being a strictly TeV-brane-localized field), but with a profile which is still peaked near the TeV brane (such that the Planck-weak hierarchy is still addressed), i.e. a ''bulk Higgs'' [26]. Moreover, the warped geometry might deviate from pure AdS near the TeV brane, which in fact could be replaced with a ''soft wall'' [27]. Similarly, in general, there are nonzero TeV-brane-localized kinetic terms for the bulk fields [28]. Such variations of the minimal models are not likely to modify the constraint on the KK mass scale from various precision tests by much more than $O(1)$ factors. However, even such modest changes can dramatically impact the LHC signals, especially the production cross sections for the KK modes.

With the above motivation, the ''two-site model'' [29] was proposed as an economical description of this framework in order to capture the robust aspects of the phenomenology by effectively restricting to the SM fields and their first KK excitations. In Ref. [30], it was shown that a mass scale for the new particles as low as $\sim O(5)$ TeV is consistent with the combination of constraints from ϵ_K and BR ($b \to s\gamma$), and it was suggested that models with a bulk Higgs can allow a similar KK scale. In addition, mechanisms exist to ameliorate such constraints in a *parametric* manner, for example, through flavor symmetries [24,31] or by lowering the UV-IR hierarchy [32], as opposed to simply relying on the $O(1)$ effects mentioned above.

Most of the studies of the KK gluon, graviton, and Z (and similarly our study of the KK W here) focus on flavor-*preserving* fermionic decays (i.e., $t\bar{t}$ for neutral and $t\bar{b}$ for charged case), except for Ref. [33] which considers flavor-*violating* decays of the KK gluon. So, it is important to point out that the results of these studies apply to the warped extra dimensional framework independent of the specific mechanism used to suppress flavor violation (beyond that from the RS-GIM mechanism) since the profiles and hence the (flavor-preserving) couplings remain (roughly) the same in all these different models for suppressing flavor violation (except in Ref. [32] with UV-IR hierarchy being smaller than Planck-weak hierarchy). For other studies of flavor physics, see Refs. [34,35].

Finally, various custodial symmetries [36,37] can be incorporated such that the constraints from the various (flavor-preserving) electroweak precision tests (EWPT) can be satisfied for a few TeV KK scale [36,38]. The bottom line is that a few TeV mass scale for the KK gauge bosons can be consistent with both electroweak and flavor precision tests.

A. Couplings

Clearly, the light fermions have a small couplings to all KK's (including the graviton) based simply on the overlaps of the corresponding profiles, while the top quark and Higgs have a large coupling to the KK's. Schematically, neglecting effects related to EWSB, we find the following ratio of RS1 to SM gauge couplings:

$$\frac{g_{\rm RS}^{q\bar{q},l\bar{l}A^{(1)}}}{g_{\rm SM}} \simeq -\xi^{-1} \approx -\frac{1}{5}, \quad \frac{g_{\rm RS}^{Q^3\bar{Q}^3A^{(1)}}}{g_{\rm SM}}, \frac{g_{\rm RS}^{t_R\bar{t}_RA^{(1)}}}{g_{\rm SM}} \simeq 1 \text{ to } \xi(\approx 5),$$
$$\frac{g_{\rm RS}^{HHA^{(1)}}}{g_{\rm SM}} \simeq \xi \approx 5 \quad (H = h, W_L, Z_L), \quad \frac{g_{\rm RS}^{A^{(0)}A^{(0)}A^{(1)}}}{g_{\rm SM}} \sim 0. \quad (1)$$

Here $q = u, d, s, c, b_R$, $l =$ all leptons, $Q^3 = (t, b)_L$, and $A^{(0)}$ ($A^{(1)}$) correspond to zero (first KK) states of the gauge fields. Also, $g_{\rm RS}^{xyz}$, $g_{\rm SM}$ stand for the RS1 and the three SM (i.e., 4D) gauge couplings, respectively. Note that H includes both the physical Higgs (h) and *unphysical* Higgs, i.e., *longitudinal* W/Z by the equivalence theorem (the derivative involved in this coupling is similar for RS1 and SM cases and hence is not shown for simplicity). Finally, the parameter ξ is related to the Planck-weak hierarchy: $\xi \equiv \sqrt{k\pi r_c}$. EWSB induces mixing between EW KK states, which we discuss in Appendix A.

For completeness, we present the couplings of the KK graviton to the SM particles. These couplings involve derivatives (for the case of *all* SM particles), but (apart from a factor from the overlap of the profiles) it turns out that this energy-momentum dependence is compensated (or made dimensionless) by the $\bar{M}_P e^{-k\pi r_c} \sim$ TeV scale, instead of the $\bar{M}_P$-suppressed coupling to the SM graviton. Again, schematically,

$$\begin{aligned} g_{\rm RS}^{q\bar{q},l\bar{l}G^{(1)}} &\sim \frac{E}{\bar{M}_P e^{-k\pi r_c}} \times \text{4D Yukawa}, \\ g_{\rm RS}^{A^{(0)}A^{(0)}G^{(1)}} &\sim \frac{1}{k\pi r_c} \frac{E^2}{\bar{M}_P e^{-k\pi r_c}}, \\ g_{\rm RS}^{Q^3\bar{Q}^3A^{(1)}}, g_{\rm RS}^{t_R\bar{t}_RG^{(1)}} &\sim \left(\frac{1}{k\pi r_c} \text{ to } 1\right) \frac{E}{\bar{M}_P e^{-k\pi r_c}}, \\ g_{\rm RS}^{HHG^{(1)}} &\sim \frac{E^2}{\bar{M}_P e^{-k\pi r_c}}. \end{aligned} \quad (2)$$

Here, $G^{(1)}$ is the KK graviton and the tensor structure of the couplings is not shown for simplicity.

Next, we briefly review earlier studies of LHC signals and give an overview of the charged electroweak gauge bosons in this scenario.

B. LHC signals

Based on these couplings, and the fact that precision electroweak and flavor constraints require the mass to be bigger than a few TeV, we are faced with the following challenges in obtaining the EW KK gauge-boson signals at the LHC from direct production of the KK modes:

(i) The cross section for production of these states is suppressed to begin with due to a small coupling to the protons' constituents, and due to the large mass.
(ii) Decays to ''golden'' channels (leptons, photons) are suppressed. Instead, the decays are dominated by the top quark and the Higgs (including longitudinal W/Z).

Also, these resonances tend to be quite broad due to the enhanced couplings to the top/Higgs.

In particular, the KK graviton, gluon, and neutral electroweak gauge bosons all have sizable BR to decay to top *pairs*. Moreover, due to the large mass (few TeV) of the KK particle, the top quarks produced in their decays are highly boosted, resulting in a high degree of collimation of the top quark's decay products. Hence it is a challenge to identify these top quarks. Nonetheless, using the techniques suggested in Refs. [8,9] (see also Refs. [39] for related studies and [40,41] for recent developments of the techniques for detecting highly boosted top quarks), discovery for the KK *gluon* up to ~4 TeV mass might be possible. However, in the case of approximately degenerate gauge KK modes, it is still difficult to extract the signal from top pairs for *electroweak* neutral KK modes. The reason is that the top pair signal from these states is swamped by the decays of the KK gluon, which has a (much) larger cross section than that of the KK electroweak neutral gauge boson due to the QCD coupling and color factors, even though the SM $t\bar{t}$ background might be smaller than the electroweak neutral KK signal.

As mentioned above, couplings of KK's to longitudinal W/Z are also enhanced similarly to top quarks (of course, only for KK graviton and electroweak—both neutral and charged—KK modes) so that decays to these modes also have a significant BR. Such final states are *a priori* cleaner than top quarks, in particular, since there is no ''pollution'' from QCD or KK gluons and since there are decay channels with no jets in these cases. Hence such final states might be the discovery modes for electroweak (both charged and neutral) and graviton KK states. However, we still face some challenges in discovering the *neutral* electroweak (cf. charged case below) and graviton KK states even with the W/Z final states, as follows. The purely leptonic decay in the WW channel has a small BR, and moreover, the WW invariant mass cannot be fully reconstructed due to the presence of missing momentum from *two* ν's. Since it is difficult then to apply the mass window cut efficiently (i.e., without reducing the signal) in order to isolate the events in the resonance region only, the SM background tends to be larger. It is true that the $ZZ \to 4l$ final state can be fully reconstructed, but it has an even smaller BR to leptons than the WW channel and is available only for the graviton (it is absent for the neutral electroweak gauge KK).

On the other hand, the semileptonic decay of the WW from the KK Z and graviton has a larger BR. However, just as for the top quarks mentioned above, the hadronic decays of the highly boosted W/Z pose a challenge for detection: the 2 jets from W/Z tend to merge so that the QCD W/Z + jet background (where a QCD jet fakes a hadronically decaying W/Z) becomes significant. Of course, this back-

ground is reducible so that with suitable discriminators between QCD and W/Z jets such as jet mass, this channel can still be useful [13]. A similar argument applies to decays of KK W to WZ.

In this paper, we study LHC signals from direct production of *charged* electroweak KK gauge bosons in the framework of a warped extra dimension. Apart from completing the study of spin-1 KK's, our motivation for this study is that these states possess some new features relative to KK *neutral* electroweak gauge bosons and gravitons:

(i) The fully leptonic (and hence clean) decay mode of the WZ channel can be fully reconstructed[1] due to the presence of only *one* ν. Hence, it is expected that the signal-to-background ratio can be enhanced efficiently by a suitable cut on the WZ invariant mass, namely, by simply requiring this mass to lie in the resonance region (unlike for the neutral case discussed above). Moreover, this final state for the WZ has a larger BR than the $ZZ \to 4l$ case for the KK graviton (although the leptonic BR of WZ is smaller than that of the fully leptonic decay of the WW final state for the KK graviton and *neutral* electroweak gauge boson).
The issues with the semileptonic decay of WZ will be similar to that in the neutral electroweak gauge-boson case.

(ii) Decays to the top + bottom final state of electroweak charged gauge bosons can also be reconstructed even for the leptonic decay mode of the top quark.[2] The irreducible SM background from the electroweak process (single-top production) can be shown to be smaller than the signal inside the resonance region. Compared to the case of the neutral electroweak KK's where the decays to top pairs have an irreducible SM background from QCD processes, the electroweak background for the charged case is smaller (and the signal cross section for the neutral case is roughly similar to the charged case). Moreover, if the KK gauge bosons are degenerate, then an even larger background from the KK-gluon decays to top pairs completely swamps the signal from the electroweak neutral KK boson.
However, even for the charged case, QCD top pairs (from the KK gluon or the SM) can be a significant background if one top quark fakes a bottom quark due to collimation of its decay products. Of course, techniques to distinguish a highly boosted top from a bottom can suppress this background; i.e., it is a *reducible* one.

[1]Assuming that the missing momentum from the neutrino combined with the lepton forms a W, or assuming that the neutrino 3-momentum is collinear with that of the lepton due to the large boost of the W in the lab frame.

[2]Imposing the on-shell conditions for M_W and m_t.

C. Overview of the charged electroweak gauge-boson sector

We present the full details on the model we work with along with a derivation of all the W' couplings in Appendixes A and B. Here, we summarize some of the salient features of the various cases that we study in detail in the next two sections. First of all, due to the extended EW gauge symmetry in the bulk, i.e., $SU(2)_L \otimes SU(2)_R \otimes U(1)_X$ which is motivated by suppressing contributions to the T parameter, we see that there are two charged KK towers [one from each $SU(2)$ group], before EWSB. We will restrict our discussion to the first mode of each tower, denoting these states by W_{L_1,R_1}, respectively. EWSB will mix these states, and the resulting mass eigenstates will be denoted by $W'_{L,R}$.

As explained above, these charged EW gauge bosons will decay mostly into Higgs, including (longitudinal) W/Z, and to top-bottom final states. In the Appendixes, we define two cases for the top-bottom sector [corresponding to different representations for the top-bottom sector under the $SU(2)_R \otimes U(1)_X$ group] that we will consider in this work. Here we summarize the main features of the two cases (details are given in the Appendixes).

Case (i): t_R has a close-to-flat profile and $(t, b)_L$ has a profile localized very close to the TeV brane in the bulk.

Case (ii): vice versa, i.e., $(t, b)_L$ has a close-to-flat profile and t_R has a profile localized very close to the TeV brane in the bulk.

Roughly speaking, flavor precision tests tend to (strongly) prefer case (ii), whereas EW precision tests have a (milder) preference for case (i).

Since, as shown in the Appendixes, the representations under $SU(2)_L \times SU(2)_R \times U(1)_X$ for these two cases are less than minimal, there are various "exotic" fermion fields included in these representations [cf. Eqs. (B1) and (B2)] in addition to the SM fermions. These non-SM fermions can be looked for at the LHC, but we will not consider them here; instead we will restrict ourselves to SM final states. However, in order to obtain realistic values, we will include these non-SM decay channels in computing the BR.

III. W' DECAYS

The W' couplings to fermions in the four-dimensional effective theory depend on the overlap of the corresponding profiles in the extra dimension, which are presented in Table X. Based on these overlap integrals and the gauge quantum numbers, we then derive the W' couplings to gauge bosons in the rest of Appendix B. Armed with these couplings, we are ready to embark on the phenomenology of charged EW gauge bosons in this framework. We have incorporated the W' couplings shown in Appendix B into the Monte Carlo program CALCHEP [42], with which we present the results below. In Fig. 1 we show the total widths

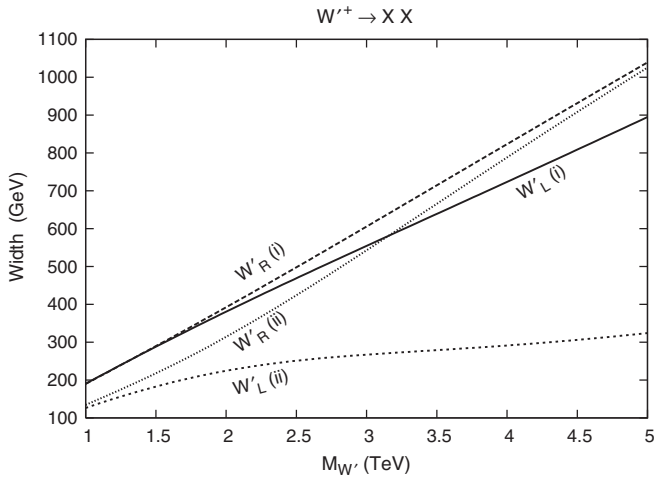

FIG. 1. The total widths of W_L' and W_R' as a function of their masses for cases (i) and (ii).

of the W_L' and W_R' into two-body final states as a function of their masses for cases (i) and (ii). The total width increases monotonically with $M_{W'}$ as expected, and is roughly about 20% or less of its mass, with it being appreciably smaller for the W_L' in case (ii). This implies a typically weakly interacting particle and a prompt decay, although the width can still be rather large for a high mass. A distinct feature is that the total width of W_L' in case (ii) is much smaller than all the other widths (for large $M_{W'}$). This is due to the fact that in case (ii) there is no direct coupling of the W_{L_1} ($\approx W_L'$ in the limit of large $M_{W'}$) to a third generation fermion whose wave function is peaked toward the TeV brane, unlike for the states in case (i) and for W_{R_1} in case (ii). This is a direct result of the $SU(2)_L \otimes SU(2)_R$ quantum numbers of the third generation fermions [cf. Eqs. (B1) and (B2)]. Note, however, that it can still be coupled to a TeV-brane peaked state via $W_{L_1} \leftrightarrow W_{R_1}$ mixing, but this would

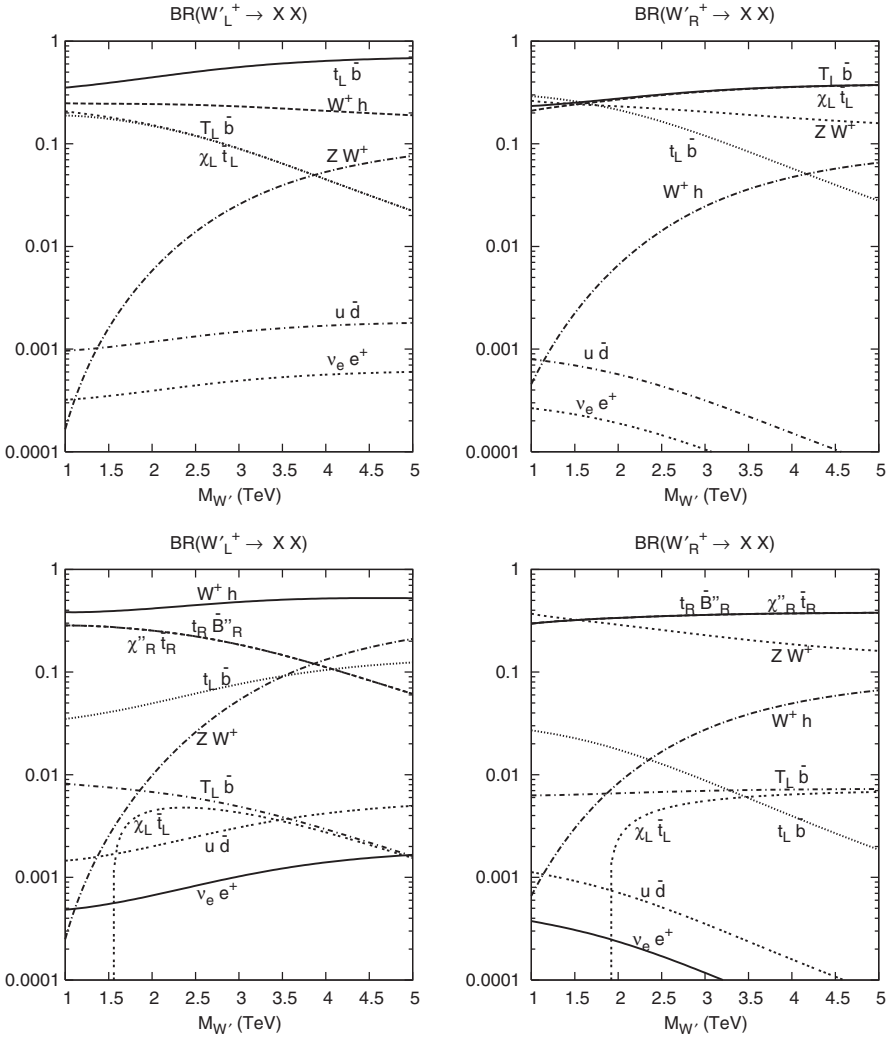

FIG. 2. The branching fractions of W_L' (left panels) and W_R' (right panels) as a function of their masses for case (i) (top panels) and case (ii) (bottom panels). In the bottom panel for case (ii), note that the curves for $t_R \bar{B}_R''$ and $\chi_R'' \bar{t}_R$ are on top of each other and cannot be individually differentiated. The χ_L, T_L, χ_R'', B_R'' are the extra non-SM fermions.

be suppressed by this mixing angle which is small for large $M_{W'}$.

In Fig. 2 we show the BR of the mass eigenstates W'_L (left panel) and W'_R (right panel) into various two-body final states for cases (i) (top panels) and (ii) (bottom panels). The largest branching fraction is to fermions peaked toward the TeV brane, which in case (i) is to Q^3_L modes, while for W'_R in case (ii) it is to the triplet containing t_R. In contrast, for the W'_L in case (ii) the largest BR is to Wh since there is no direct coupling to a third generation fermion with a TeV-brane peaked profile. For the W'_R in case (ii), the ZW final state is also available with a sizable BR. In case (ii) the $\chi_L \bar{t}_L$ is available only for $M_{W'} > M_{\chi_L} + M_t$, and therefore exhibits a threshold behavior, where χ_L is a non-SM fermion.

In this work we do not study the non-SM fermions in the final states, and we will focus on the $t\bar{b}$, ZW, and Wh final states in the rest of the paper. The BR into the $\ell\nu$ final state is tiny, but due to its uniqueness and for completeness, we will briefly comment on this mode also. We will perform a detailed study of these final states, considering their various decay modes, and obtain the LHC reach.

IV. CHARGED GAUGE-BOSON SIGNALS AT THE LHC

In this section we consider the production of the charged KK gauge bosons (generically denoted by W') and their decay into various SM final states at the LHC. We first present in Fig. 3 the total production cross section for the W' at the LHC versus its mass $M_{W'}$ via the Drell-Yan (DY) process. We see that the cross section can be $100 - 1$ fb for $M_{W'} = 2$–4 TeV. The W'_R coupling to light quarks is suppressed by the $W_{L_1} \leftrightarrow W_{R_1}$ mixing angle [cf. Eq. (B3)] and the rate is therefore smaller by a factor of 2–10 in the mass range mentioned above. In the following analyses, we coherently sum the W'_L and W'_R (the mass eigenstates) contributions. There are other possible mechanisms for W' production. One may consider the gauge-boson fusion $WZ \to W'$. However, the gauge-boson fusion channel, as first explored in [13], was found to be subleading. As mentioned earlier, we adopt the Monte Carlo package CALCHEP [42] to obtain the numerical results in this section. We use the CTEQ6M for parton distribution functions [43].

A. $t\bar{b}$ final state

We first consider the production and decay channel

$$pp \to W'^{+} \to t\bar{b} \quad \text{with} \quad t \to b\ell\bar{\nu} \qquad (\ell = e, \mu), \tag{3}$$

where the leptonic decay modes of the top have been specified for the purpose of event triggering and identification. The most distinctive feature of this signal is the large invariant mass of the tb system near $M_{W'}$. Although the missing neutrino makes the event reconstruction less trivial, one should be able to reconstruct the neutrino momentum fairly effectively by demanding the two mass relations $M_W^2 = (p_l + p_\nu)^2$, $m_t^2 = (p_b + p_l + p_\nu)^2$. We thus assume that the signal events are fully reconstructible.

We select events with the basic acceptance cuts

$$|y_{W,b,\bar{b}}| < 3; \qquad p_{TW,b,\bar{b}} > 50 \text{ GeV}, \tag{4}$$

where the y's are the rapidities. For the signal events from a heavy W' decay, further tightened cuts can help for the background suppression. We thus impose the cuts on the top and b quarks,

$$p_{Tt,b} > 200 \text{ GeV}, \qquad |y_{t,b}| < 3. \tag{5}$$

In Fig. 4, we present the differential distributions for the $t\bar{b}$ final state with a variety of values of $M_{W'} = 2$, 3, and 4 TeV, for (a) the transverse momentum distribution and (b) the transverse mass distribution. Also shown on the figures is the dominant source of irreducible background, the SM single-top production $pp \to W^+ \to t\bar{b}$, seen as the continuum curves. We see the very promising prospects for observing the signal with suitably chosen cuts.

With the decay of the top (into Wb), the SM $Wb\bar{b}$ will be an additional source of background. Since this background largely populates the low mass threshold region, we thus form the following cluster transverse mass to help distinguish the signal from the background,

$$M_{TWb} = \left(\sqrt{p_{TW}^2 + m_W^2} + p_{Tb}\right)^2 - |\mathbf{p}_{T_W} + \mathbf{p}_{T_b}|^2,$$
$$M_{TWb\bar{b}} = p_{Tb} + p_{T\bar{b}} + \sqrt{p_{TW}^2 + m_W^2}. \tag{6}$$

We show the representative kinematical distributions for

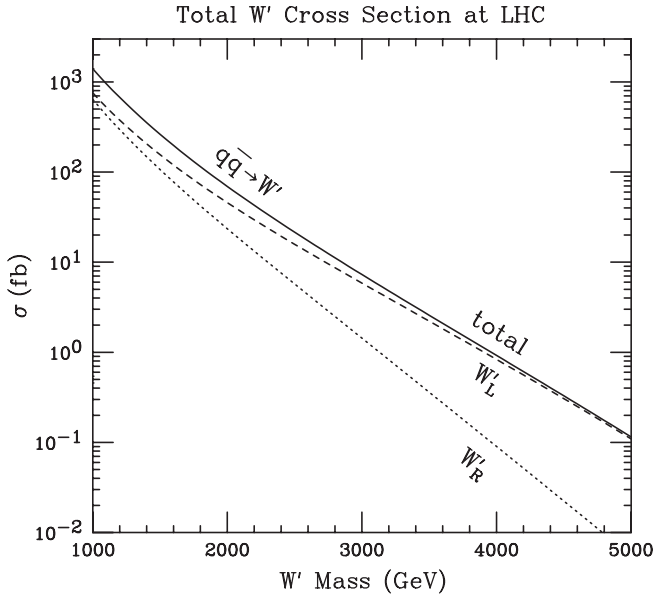

FIG. 3. Total production cross section for W' versus its mass at the LHC.

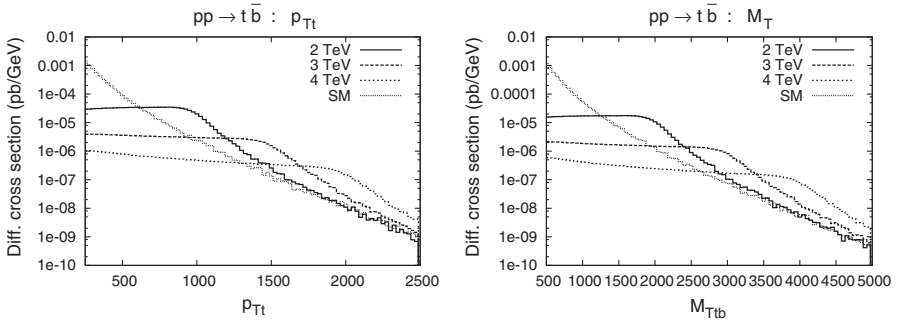

FIG. 4. The p_{Tt} (left panel) and M_{Ttb} (right panel) differential distributions of the process $pp \to W'^{+} \to t\bar{b}$ for $M_{W'} = 2$, 3, and 4 TeV for case (i). These are after the cuts in Eq. (5). Also shown are the SM single-top background distributions.

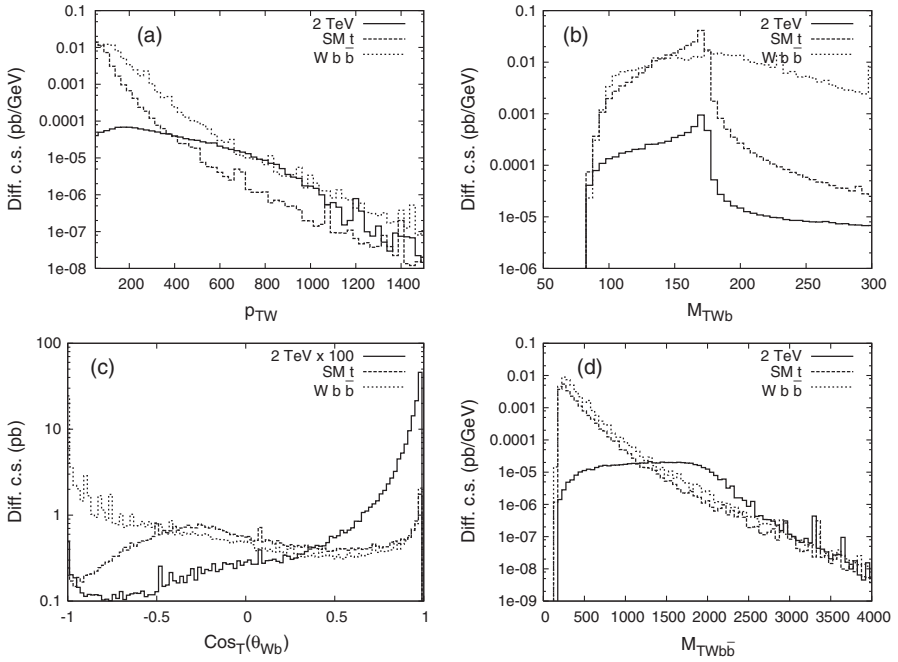

FIG. 5. The p_{TW} (top-left panel), M_{TWb} (top-right panel), $\cos_T\theta_{Wb}$ (bottom-left panel), and $M_{TWb\bar{b}}$ (bottom-right panel) differential distributions of the process $pp \to W^{+}b\bar{b}$ for $M_{W'} = 2$ TeV, for case (i). Also shown are the irreducible backgrounds, the SM single-top $t\bar{b}$ and $Wb\bar{b}$.

the $Wb\bar{b}$ final states in Fig. 5, with an $M_{W'} = 2$ TeV signal (solid curves) for illustration. The SM backgrounds of $t\bar{b}$ (dashed lines) and $Wb\bar{b}$ (dotted lines) are also shown for comparison. Figure 5(a) presents the transverse momentum distribution for the W. In Fig. 5(b), we show the distribution of M_{TWb}, the cluster transverse mass of the W with the nearer of the two b jets. The top-quark mass reconstruction is visible for those events with a real top in the final state. We show in Fig. 5(c) the distribution of $\cos_T\theta_{Wb}$, the cosine of the angle in the transverse plane between the W and the nearer of the two b jets. Because of the large boost of the top quark from the W' decay for the signal, the opening angle obviously is rather small as seen by the solid curve. In Fig. 5(d), we show the distribution of the full transverse mass of the $Wb\bar{b}$ system. It is encouraging to see a possible separation of the signal from the backgrounds.

Since there is only one missing neutrino, the kinematical variables can be fully reconstructed in the event as discussed earlier by demanding the mass reconstruction of M_W, m_t. Alternatively, since the W is produced with a large boost, the neutrino will be considerably collimated with the charged lepton. If one makes the assumption[3] $\vec{p}_\nu \approx \kappa\vec{p}_\ell$, the neutrino 4-momentum can be approximately determined and the full $M_{Wb\bar{b}}$ can be formed. We find that doing so gives a narrower signal invariant-mass peak, but also raises the background in the region of interest, resulting in a marginal improvement in significance; we therefore do not pursue either of these ideas here.

The distributions in Fig. 5 motivate us to consider the following cuts:

[3]Practically, $p_T(\nu) = \not{E}_T$, $p_L(\nu) = p_L(\ell) \times \frac{\not{E}_T}{p_T(\ell)}$.

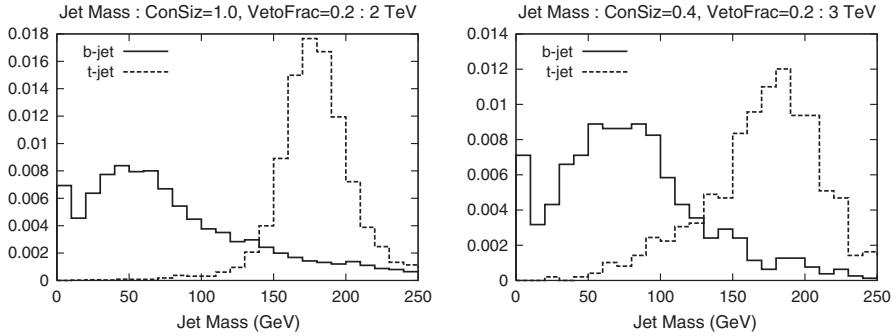

FIG. 6. The jet-mass distributions for top and bottom jets. These are after basic, Wb, and invariant-mass cuts. The left panel is for 2 TeV with cone size 1.0, and the right panel is for 3 TeV with cone size 0.4. Both are with a veto fraction of 0.2.

M_{TWb} cut: $100 < M_{TWb} < 190$ GeV, since we expect that for the signal this should reconstruct to the parent $m_{\rm top}$, as can be seen in Fig. 5(b). Notice that since for the single top this also reconstructs to $M_{\rm top}$, this variable does not discriminate between the signal and this source of background.

Wb angle cut: $\cos_T\theta_{Wb} > 0.5$, motivated from (c), where we see that for the signal, the Wb opening angle is fairly small owing to the large boost of the parent top.

$2b$ tags: We demand that there be two tagged b's in the event. We adopt a b-tagging efficiency $\eta_b = 0.4$ [44]. With b-tagging parameters optimized for low p_{Tb}, the light-quark rejection ratio (for $j = u, d, s, g$) is roughly $R_j = 20$ [44], where $1/R_j$ is the probability of mistaking a light jet for a b jet. We believe this is likely to be improved with tagging techniques optimized for high p_{Tb}, and since our light-quark jet background is significant, we anticipate such improvements and use $R_j = 40$. We use a charm quark rejection factor $R_c = 5$.

M_{TWbB} cut: $1500 < M_{TWb\bar{b}} < 2500$ GeV (for $M_{W'} = 2$ TeV) and $2400 < M_{TWb\bar{b}} < 3600$ GeV (for $M_{W'} = 3$ TeV), which is motivated by the resonant feature of the signal as seen clearly in (d), and results in the background being very effectively suppressed after this cut.

Jet-mass cut: $t\bar{t}$ production can become a source of background since a top can fake a b jet, for instance, when the hadronic decay products of a boosted top are sufficiently collimated that it can be confused for a b jet. The two main sources of a top pair are the SM QCD production, and the KK-gluon production which dominantly decays to this channel. Both can be significantly larger than the signal, and the latter is especially problematic since it is resonant in the same invariant-mass region as the signal. However, the jet-mass variable can be used to discriminate between a b jet and a boosted hadronic top, with the distributions expected to peak at m_b and m_t, respectively. In order to obtain a rough estimate of the separation achievable, we have used PYTHIA V6.411 [45] to shower a bottom and a hadronically decayed top, followed by smearing the daughter particle's energy by $80\%/\sqrt{E}$, and η and ϕ by 0.05 to mimic the finite resolutions of the detector.[4] In general, a larger cone size will include more of the radiation and results in a narrower distribution for t jets but at the expense of moving the b-jet peak to larger values. Also, since a b jet is expected to be more collimated than a t jet, we also demand that 80% of the p_T be contained within the cone (veto fraction of 0.2). We show in Fig. 6 the resulting jet-mass distributions for the 2 TeV (left panel) and 3 TeV (right panel) cases. For the 2 TeV case, we find a cone size of 1.0 to result in adequate separation, and a jet-mass cut $M_j < 75$ GeV with a veto fraction of 0.2 retains 46% of b jets and 0.38% of t jets. For the 3 TeV case, the decay products are more collimated and we therefore pick a smaller cone size, namely, 0.4, and again with a veto fraction of 0.2. We find that, with the cut $M_j < 100$ GeV (larger than the previous case in order to keep more of the already small signal events), 57% of b jets and 2.5% of t jets are retained.

In Table I we present the signal and background cross sections (in fb) for the process $pp \to Wb\bar{b} \to \ell\nu b\bar{b}$ for case (i). We include in the signal both W'^+ and W'^-, and we find that the latter cross section is about a third of the former, stemming from the difference in the parton distribution functions of more u quarks than d quarks in a proton. We count for both $\ell = e, \mu$. Because of the large boost of the parent top, the lepton may not have a large isolation with respect to the b jet, but we will assume that this will not result in too large a loss of efficiency. Ways to deal with this have been discussed in Refs. [8,40]. The entry labeled as "SM top," in addition to the SM $W^{\pm}$-exchange single-top process, also includes the W-glue fusion process containing an extra jet that we use to veto events with $p_{Tj} > 20$ GeV in the central region. In the last two columns we show the significance without and with $t\bar{t}$ as a source of background, with the significance including the latter shown in parentheses. The significance

[4]We are grateful to Frank Paige for many discussions on jet-mass issues. This variable was also explored in Ref. [13] for the jet mass of the W. Related issues, including using jet substructure to discriminate between highly boosted W/top and QCD jets, have also been discussed in Refs. [9,40,41,46].

TABLE I. The cross sections (in fb) for the signal process $pp \to W' \to tb \to W\bar{b}b \to \ell\nu\bar{b}b$ for case (i), and the SM background, with the cuts applied successively. Cross sections are shown for $M_{W'} = 2$ and 3 TeV, with the number of events and significance for $\mathcal{L} = 100$ and 300 fb^{-1}, respectively. In the last two columns we show the significance (S_σ) without and with $t\bar{t}$ as a source of background, with the significance including the latter shown in parentheses.

2 TeV, 100 fb^{-1}	Basic	Wb cuts	b tag	M_{TWbb}	M_j	Number of events	S/B	S_σ
Case (i)	8.9	7	1.1	0.44	0.2	20	2.5 (1.4)	7(5,3)
SM top	1400	370	60	0.09	0.04	4		
SM $Wb\bar{b}$	520	66	11	9×10^{-3}	4×10^{-3}	0.4		
SM Wbj	9×10^3	2×10^3	20	0.04	0.02	2		
SM Wcj	4×10^3	700	4	10^{-3}	0.5×10^{-3}	0.05		
SM Wjj	2×10^5	2×10^4	13	0.03	0.01	1		
SM $t\bar{t}$	4×10^4	10^4	2×10^3	4.5	0.02	2		
$G^{(1)}$ $t\bar{t}$ (i)	250	190	30	10	0.04	4		

3 TeV, 300 fb^{-1}	Basic	Wb cuts	b tag	M_{TWbb}	M_j	Number of events	S/B	S_σ
Case (i)	1.5	1.1	0.18	0.04	0.02	7	5.8 (0,9)	4.5(2.2)
SM top	1400	370	60	4×10^{-3}	2×10^{-3}	0.6		
SM $Wb\bar{b}$	520	66	11	4×10^{-4}	2.3×10^{-4}	0.07		
SM Wbj	9×10^3	2×10^3	20	10^{-3}	0.5×10^{-3}	0.2		
SM Wcj	4×10^3	700	4	10^{-4}	0.5×10^{-4}	0.02		
SM Wjj	2×10^5	2×10^4	13	2×10^{-3}	10^{-3}	0.3		
SM $t\bar{t}$	4×10^4	10^4	2×10^3	0.21	5.3×10^{-3}	1.6		
$G^{(1)}$ $t\bar{t}$ (i)	32	24	4	0.64	0.02	5		

is computed as $S_\sigma = S/\sqrt{B}$, but when the number of events is small, we use Poisson statistics and quote an equivalent Gaussian significance. The $G^{(1)}$ (KK gluon) is taken to be degenerate with W'. From the table we see that we need $\mathcal{L} = 100$ fb^{-1} ($\mathcal{L} = 300$ fb^{-1}) for a 2 TeV (3 TeV) W'. Although the S/B is good for heavier masses, the signal will still be limited by statistics.

In Table II we present the signal and background cross sections (in fb) for the process $pp \to Wb\bar{b} \to \ell\nu b\bar{b}$ for case (ii). Rather than repeating, in Table II we have combined, in SM Wj_1j_2, the SM $Wb\bar{b}$, Wbj, Wcj, and Wjj channels shown separately in Table I. Compared to case (i), as expected, the cross section is lower in case (ii) since the t_L, b_L profiles are not peaked near the TeV brane (and hence do not have as large a coupling to W') as in the former case. Although the t_R is peaked near the TeV brane in case (ii), it either does not couple to W' if it is an $SU(2)_R$ singlet, or would couple to it only associated with a non-SM fermion if it is a triplet. We find that we need a much higher luminosity, namely, 1000 fb^{-1} for a 2 TeV W'. In this case, we expect the other channels (to be discussed in the following) to have better reach.

B. ZW final state

As for the process

$$pp \to W' \to ZW, \tag{7}$$

we consider separately the various decay modes of the Z and W. We do not pursue the $Z \to \nu\nu$ decay channel in which we cannot reconstruct the event even in the transverse plane. Although *simultaneous* hadronic decays of Z and W have the largest branching fraction, the multiple jet background from QCD would be overwhelming. We therefore do not pursue this mode in our study.

Since there is at most one missing neutrino in the final state, we can reconstruct the event if one makes the as-

TABLE II. The cross sections (in fb) for the signal process $pp \to W' \to tb \to W\bar{b}b \to \ell\nu\bar{b}b$ for case (ii), and the SM background, with the cuts applied successively. Cross sections are shown for $M_{W'} = 2$ TeV, with the number of events and significance for $\mathcal{L} = 1000$ fb^{-1}. In the last two columns we show the significance (S_σ) without and with $t\bar{t}$ as a source of background, with the significance including the latter shown in parentheses.

2 TeV	Basic	Wb cuts	b tag	M_{TWbb}	M_j	Number of events	S/B	S_σ
Case (ii)	0.75	0.6	0.1	0.05	0.03	30	0.38 (0.2)	3.4 (2.5)
SM top	1400	370	60	0.09	0.04	40		
SM Wj_1j_2	2.1×10^5	2.2×10^4	48	0.08	0.04	40		
SM $t\bar{t}$	4×10^4	10^4	2×10^3	4.5	0.02	20		
$G^{(1)}$ $t\bar{t}$ (ii)	210	180	29	13	0.05	50		

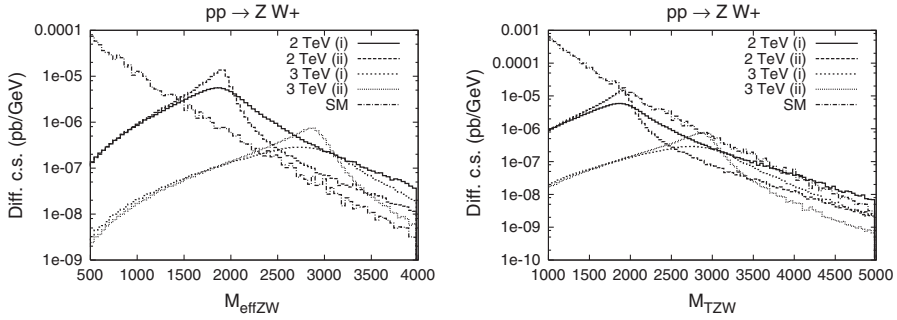

FIG. 7. The $M_{\mathrm{eff}_{ZW}}$ (left panel) and $M_{T_{ZW}}$ (right panel) distributions for signal and SM background for the process $pp \to ZW^+$ after the cuts $p_{TZ,W} > 100$ GeV and $|y_{Z,W}| < 3$. Both case (i) and case (ii) are shown.

sumption $\vec{p}_\nu \approx \kappa \vec{p}_e$ (see the discussions in the last section). On the other hand, it is more straightforward to construct the events in the transverse plane. For illustration, we form the following kinematic variables:

$$M_{\mathrm{eff}_{ZW}} = p_{TZ} + p_{TW}, \tag{8}$$

$$M_{T_{ZW}} = \sqrt{p_{TZ}^2 + M_Z^2} + \sqrt{p_{TW}^2 + M_W^2}. \tag{9}$$

In Fig. 7 we show the $M_{\mathrm{eff}_{ZW}}$ and $M_{T_{ZW}}$ differential distributions for the process $pp \to ZW^+$ for the W' signal for cases (i) and (ii), and the irreducible SM WZ background.

1. Fully leptonic channel

In the fully leptonic final state we consider the process $pp \to W' \to ZW$ followed by $Z \to \ell\ell$ and $W \to \ell\nu$. We take into account the SM ZW going into the same final state as the main source of (irreducible) background. We select events with the basic cuts

$$p_{T\ell} > 50 \text{ GeV}; \qquad p_{T\mathrm{miss}} > 50 \text{ GeV}; \qquad |\eta_\ell| < 3. \tag{10}$$

In addition to the basic cuts, we apply the following cuts sequentially in order to optimally improve signal observation from the background.

M_{eff} cut: $M_{\mathrm{eff}} > 1$ TeV (for $M_{W'} = 2$ TeV) and $M_{\mathrm{eff}} > 1.25$ TeV (for $M_{W'} = 3$ TeV).

M_T cut: $1.5 < M_{T_{ZW}} < 2.5$ TeV (for $M_{W'} = 2$ TeV) and $2.4 < M_{T_{ZW}} < 3.6$ TeV (for $M_{W'} = 3$ TeV).

In Table III we show the cross sections (in fb) for the fully leptonic signal and background for case (i) and case (ii) with the above cuts applied. Given the small BR into this final state, it is not surprising that we will need a large luminosity to see this signal. The fully leptonic mode is experimentally clean. The significance is computed as $S_\sigma = S/\sqrt{B}$, but when the number of events is small, we use Poisson statistics and quote an equivalent Gaussian significance. We find that we need $\mathcal{L} = 100$ fb^{-1} ($\mathcal{L} = 1000$ fb^{-1}) for a 2 TeV (3 TeV) W' to reach a statistically significant signal. We turn next to the semileptonic mode which has a larger BR and therefore a larger rate.

2. Semileptonic channel

We consider below the signal identification in the two semileptonic modes $Z \to \ell\ell$, $W \to jj$ and $Z \to jj$, $W \to \ell\nu$. As explained in detail in Ref. [13], the two jets may merge into one fat jet due to the large boost of the parent gauge boson, picking up a one-jet background (in addition to the already mentioned SM ZW background).

$Z \to \ell\ell, W \to jj$: Since there is no missing energy in the event, we can reconstruct the event fully and form the full

TABLE III. The cross sections (in fb) for the signal process $pp \to W' \to ZW \to \ell\ell\ell\nu$ for case (i) and case (ii), and the SM background, with the cuts applied successively. We show cross sections for $M_{W'} = 2$ and 3 TeV, and the number of events and significance (S_σ) with the luminosity $\mathcal{L}$ (in fb^{-1}) as shown for each case.

2 TeV	Basic	M_{eff}	M_T	$\mathcal{L}$	Number of events	S/B	S_σ
Case (i)	0.13	0.13	0.1	100	10	5	5.1
Case (ii)	0.17	0.16	0.13	100	13	6.5	6.1
SM ZW	42	0.16	0.02		2		

3 TeV	Basic	M_{eff}	M_T	$\mathcal{L}$	Number of events	S/B	S_σ
Case (i)	0.01	0.01	0.006	1000	6	6	4.3
Case (ii)	0.014	0.01	0.01	1000	10	10	6
SM ZW	42	0.05	0.001		1		

TABLE IV. The cross sections (in fb) for the signal process $pp \to W' \to ZW \to \ell\ell jj$ for case (i) and case (ii), and the SM background, with the cuts applied successively. We show cross sections for $M_{W'} = 2$ and 3 TeV, and the number of events and significance (S_σ) with the luminosity $\mathcal{L}$ (in fb^{-1}) as shown for each case.

2 TeV	Basic	$M_{\rm eff}$	$M_{\rm inv}$	M_j	$\mathcal{L}$	Number of events	S/B	S_σ
Case (i)	0.4	0.4	0.16	0.13	1000	130	0.2	5
Case (ii)	0.5	0.48	0.38	0.3	300	90	0.5	6.4
SM ZW	130	0.5	0.05	0.04		40, 12		
SM $Z + 1j$	3600	63	2.1	0.63		630, 190		

3 TeV	Basic	$M_{\rm eff}$	$M_{\rm inv}$	M_j	$\mathcal{L}$	Number of events	S/B	S_σ
Case (i)	0.03	0.03	0.01	⋯	1000	10	0.07	0.8
Case (ii)	0.04	0.04	0.03	⋯	1000	30	0.22	2.6
SM ZW	130	0.16	0.006	⋯		6		
SM $Z + 1j$	3600	25	0.13	⋯		130		

invariant mass ($M_{\rm inv}$, not just M_T). In addition to the SM ZW background, due to jet merging, we have to contend with the $Z + 1$ jet as a source of background. We apply the following cuts to maximize the signal significance:

Basic cuts: $p_{T\ell} > 250$ GeV; $p_{Tj} > 500$ GeV; $|\eta_\ell| < 2$; $|\eta_j| < 2$.

$M_{\rm eff}$ cut: $M_{\rm eff} > 1$ TeV (for $M_{W'} = 2$ TeV) and $M_{\rm eff} > 1.25$ TeV (for $M_{W'} = 3$ TeV).

$M_{\rm inv}$ cut: $1.85 < M_{ZW} < 2.15$ TeV (for $M_{W'} = 2$ TeV) and $2.8 < M_{ZW} < 3.2$ TeV (for $M_{W'} = 3$ TeV).

Jet-mass cut: $75 < M_j < 125$ GeV.

In Table IV we show the cross sections as we apply the above cuts successively.

$Z \to jj$, $W \to \ell\nu$: In addition to the SM ZW background, due to jet merging, we have to contend with the $W + 1$ jet as a source of background. We apply the following cuts to maximize significance:

Basic cuts: $p_{T\ell} > 50$ GeV; $\not{E}_T > 50$ GeV; $|\eta_\ell| < 1$; $|\eta_j| < 1$.

$M_{\rm eff}$ cut: $M_{\rm eff} > 1$ TeV (for $M_{W'} = 2$ TeV) and $M_{\rm eff} > 1.25$ TeV (for $M_{W'} = 3$ TeV).

M_T cut: $1.8 < M_{T_{ZW}} < 2.2$ TeV (for $M_{W'} = 2$ TeV) and $2.8 < M_{T_{ZW}} < 3.2$ TeV (for $M_{W'} = 3$ TeV).

Jet-mass cut: $75 < M_j < 125$ GeV.

In Table V we show the cross sections as we apply the above cuts successively, and the significance $S_\sigma = S/\sqrt{B}$.

In the semileptonic channels presented above, we find for a 2 TeV W' that we need luminosities of $\mathcal{L} = 1000$ fb^{-1} and $\mathcal{L} = 300$ fb^{-1} for cases (i) and (ii), respectively. We thus see that the tb final state discussed earlier, which requires about 100 fb^{-1}, offers a more promising channel for the W' signal observation for case (i) as compared to the semileptonic W/Z channels. For a 3 TeV W' we find that the QCD background is substantial and the signal-to-background ratio is at a level of a few percent, rendering the signal observation unlikely. Techniques to beat down this reducible QCD background can be beneficial here.

The semileptonically decaying neutral electroweak KK gauge boson (Z') also decays into the $jj\ell\nu$ final state, and its detectability has already been discussed in Ref. [13].

TABLE V. The cross sections (in fb) for the signal process $pp \to W' \to ZW \to jj\ell\not{E}_T$ for case (i) and case (ii), and the SM background, with the cuts applied successively. We show cross sections for $M_{W'} = 2$ and 3 TeV, and the number of events and significance (S_σ) with the luminosity $\mathcal{L}$ (in fb^{-1}) as shown for each case.

2 TeV	Basic	$M_{\rm eff}$	M_T	$M_{\rm jet}$	$\mathcal{L}$	Number of events	S/B	S_σ
Case (i)	1	1	0.38	0.3	1000	300	0.1	5.3
Case (ii)	1.3	1.2	0.64	0.5	300	150	0.16	4.9
SM ZW	320	1.2	0.04	0.03		30, 9		
SM $W + 1j$	3.1×10^4	220	10.5	3.2		3200, 950		

3 TeV	Basic	$M_{\rm eff}$	M_T	$M_{\rm jet}$	$\mathcal{L}$	Number of events	S/B	S_σ
Case (i)	0.08	0.08	0.016	⋯	1000	16	0.02	0.6
Case (ii)	0.1	0.1	0.04	⋯	1000	40	0.06	1.5
SM ZW	320	0.4	0.002	⋯		2		
SM $W + 1j$	3.1×10^4	89	0.68	⋯		680		

C. Wh final state

Similar to the study in the last section, we again first form the following kinematic variables in order to help separate the signal from the background:

$$M_{\mathrm{eff}Wh} = p_{TW} + p_{Th}, \tag{11}$$

$$M_{TWh} = \sqrt{p_{TW}^2 + M_W^2} + \sqrt{p_{Th}^2 + M_h^2}. \tag{12}$$

In Fig. 8 we show the $M_{\mathrm{eff}Wh}$ and M_{TWh} differential distributions for the process $pp \to W^+h$ for the W' signal for cases (i) and (ii), and the irreducible SM Wh background. We see that the signal stands comfortably over the background, and with suitably chosen cuts, we expect to obtain a good significance. Since M_h is unknown, we will take two representative cases: $M_h = 120$ GeV and 150 GeV. In the former case the dominant decay mode of the h will be to $b\bar{b}$, while in the latter, to W^+W^-. We will consider each of these cases in turn.

We would like to note that we do not consider these channels as Higgs boson discovery channels. Instead, we should consider them as case studies for illustration since we should have the knowledge about the Higgs properties when our proposed searches are undertaken at the LHC.

1. $M_h = 120$ GeV: $h \to b\bar{b}$, $W \to \ell\nu$

For this case with a relatively low mass, we estimate that $\mathrm{BR}(h \to b\bar{b}) \approx 0.7$. Because of collimation of the decay products of the Higgs, the two b jets could merge, and we therefore pick up the $W + 1$ jet as a source of background. We apply the following cuts to maximize significance:

Basic cuts: $p_{T\ell} > 50$ GeV; $\not{E}_T > 50$ GeV; $p_{T(bb)} > 100$ GeV; $|\eta_\ell| < 1$; $|\eta_j| < 1$.

M_{eff} cut: $M_{\mathrm{eff}} > 1$ TeV (for $M_{W'} = 2$ TeV) and $M_{\mathrm{eff}} > 1.25$ TeV (for $M_{W'} = 3$ TeV).

M_T cut: $1.8 < M_{TWh} < 2.2$ TeV (for $M_{W'} = 2$ TeV) and $2.8 < M_{TWh} < 3.2$ TeV (for $M_{W'} = 3$ TeV).

b-tag: Because of collimation, we may not be able to resolve the two b jets, and we therefore demand only one b tag. The efficiency for at least one tagged b is $\epsilon_b * (2 - \epsilon_b)$. Here, we take the light-jet rejection ratio $R_j = 20$, which, as noted earlier, will likely be improved upon.

In addition to the above cuts, we could apply a jet-mass cut on the collimated b-jet system, which will peak around M_h and can be used to distinguish it from a light jet. Doing so would improve the significance over that shown here.

In Table VI we show the cross sections as we apply the above cuts successively. We also show the significance computed as $S_\sigma = S/\sqrt{B}$, but when the number of events is small, we use Poisson statistics and quote an equivalent Gaussian significance. As expected, we find a better significance for case (ii) since the BR is larger. We will need $\mathcal{L} = 100$ fb^{-1} ($\mathcal{L} = 300$ fb^{-1}) for a 2 TeV (3 TeV) W' to reach a good statistical significance. Improving the b-tagging performance (by achieving larger R_j) will help reduce the $W + 1$ jet background and will make the significance better.

2. $M_h = 150$ GeV: $h \to WW \to \ell\nu jj$, $W \to jj$

For this case with a higher mass, we estimate that $\mathrm{BR}(h \to WW) \approx 0.7$. Because of collimation of the jets from the W, we will not demand that separate jets be reconstructed, but rather treat it as a single jet. We will refer to the merged jet closer to the leptonic W as the near jet j_N and the merged jet on the other side as the far jet j_F.

We require that there be a jet close to the lepton with $\Delta_{\ell j_N} < 0.9$, and we require M_{TWj_N} to be around M_h, which will reduce the $W + 2j$ background. In addition to the irreducible SM Wh background, SM $h + 1j$ also remains as a background, which we will include. In order to differentiate between a light jet and the W jet, we will apply the jet-mass cut as explained in Ref. [13].

We apply the following cuts to maximize significance:

Basic cuts: $p_{T\ell} > 25$ GeV; $\not{E}_T > 25$ GeV; $p_{Tj_N} > 50$ GeV; $p_{Tj_F} > 100$ GeV; $|\eta_\ell| < 3$; $|\eta_{j_N}| < 3$; $|\eta_{j_F}| < 3$.

M_{eff} cut: $M_{\mathrm{eff}} > 1$ TeV (for $M_{W'} = 2$ TeV) and $M_{\mathrm{eff}} > 1.25$ TeV (for $M_{W'} = 3$ TeV).

M_T cuts: $100 < M_{TWj_N} < 190$ GeV (around M_h); $1.8 < M_{TWj_Nj_F} < 2.2$ TeV (for $M_{W'} = 2$ TeV) and $2.8 < M_{TWj_Nj_F} < 3.2$ TeV (for $M_{W'} = 3$ TeV).

Jet-mass cut: $75 < M_j < 125$ GeV, on both j_N and j_F for $M_{W'} = 2$ TeV, with an acceptance of 0.87 for the W jet

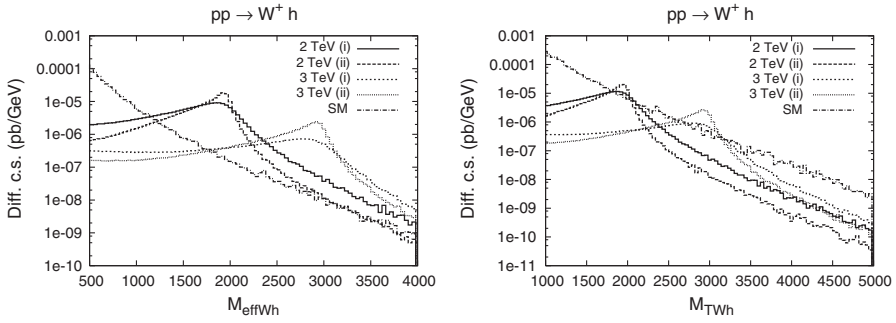

FIG. 8. The $M_{\mathrm{eff}Wh}$ (left panel) and M_{TWh} (right panel) distributions for signal and SM background for the process $pp \to W^+h$ after the cuts $p_{TW,h} > 100$ GeV and $|y_{W,h}| < 3$. Both case (i) and case (ii) are shown.

TABLE VI. The cross sections (in fb) for the signal process $pp \to W' \to Wh \to \ell \not{E}_T b\bar{b}$ for case (i) and case (ii), and the SM background, with the cuts applied successively. We show cross sections for $M_{W'} = 2$ and 3 TeV, and the number of events and significance (S_σ) with the luminosity $\mathcal{L}$ (in fb^{-1}) as shown for each case.

2 TeV	Basic	$M_{\rm eff}$	M_T	b tag	$\mathcal{L}$	Number of events	S/B	S_σ
Case (i)	1.8	1.5	0.55	0.35	100	35	0.65	4.8
Case (ii)	1.6	1.5	0.8	0.5	100	50	1	6.4
SM Wh	43	0.35	0.016	0.01		1		
SM $W + 1j$	3.1×10^4	220	10.5	0.53		53		

3 TeV	Basic	$M_{\rm eff}$	M_T	b tag	$\mathcal{L}$	Number of events	S/B	S_σ
Case (i)	0.26	0.19	0.04	0.03	300	9	1	2.75
Case (ii)	0.33	0.3	0.12	0.08	300	24	2.4	6.2
SM Wh	43	0.13	0.001	6×10^{-4}		0.2		
SM $W + 1j$	3.1×10^4	89	0.68	0.03		9		

TABLE VII. The cross sections (in fb) for the signal process $pp \to W' \to Wh \to (jj)WW \to (jj)\ell \not{E}_T(jj)$ for case (i) and case (ii), and the SM background, with the cuts applied successively. We show cross sections for $M_{W'} = 2$ and 3 TeV, and the number of events and significance (S_σ) with the luminosity $\mathcal{L}$ (in fb^{-1}) as shown for each case.

2 TeV	Basic	$M_{\rm eff}$	M_T	$M_{\rm jet}$	$\mathcal{L}$	Number of events	S/B	S_σ
Case (i)	1.6	1.3	0.43	0.34	100	34	4	8.5
Case (ii)	2.1	1.9	0.9	0.7	100	70	7	14
SM Wh	26	0.31	0.014	0.01		1		
SM $h + 1j$	220	2	0.07	0.02		2		
SM $W + 2j$	3×10^4	36	0.62	0.06		6		

3 TeV	Basic	$M_{\rm eff}$	M_T	$M_{\rm jet}$	$\mathcal{L}$	Number of events	S/B	S_σ
Case (i)	0.22	0.17	0.04	0.035	300	11	2	4
Case (ii)	0.3	0.26	0.1	0.09	300	27	4	8
SM Wh	26	0.12	8×10^{-4}	7×10^{-4}		0.2		
SM $h + 1j$	220	0.72	5×10^{-3}	2×10^{-3}		0.6		
SM $W + 2j$	3×10^4	4.1	0.05	0.015		4.5		

and 0.3 for a light jet [13]. For $M_{W'} = 3$ TeV, we apply the jet-mass cut only on j_N since its performance in j_F might deteriorate owing to increased collimation.

In Table VII we show the cross sections as we apply the above cuts successively. Similar to the previous case, we find that we will need $\mathcal{L} = 100$ fb^{-1} ($\mathcal{L} = 300$ fb^{-1}) for a 2 TeV (3 TeV) W' to reach a good statistical significance. The S/B is found to be quite adequate for a signal discovery, and the reach is limited by signal statistics.

D. $W' \to \ell\nu$ final state

In spite of the unique signal kinematics, we expect the signal event rate to be quite small for this final state, given the tiny branching ratio for this mode. Nevertheless, for completeness, we show in Table VIII for $M_{W'} = 2$ TeV the cross sections for this mode after the following cuts:

Basic cuts: $p_{T\ell} > 100$ GeV; $\not{E}_T > 100$ GeV; $|\eta_\ell| < 3$.

$M_{\rm eff}$ cut: $M_{\rm eff} > 1$ TeV.

M_T cut: $1.5 < M_{T\ell\nu} < 2.5$ TeV.

We include the SM $W^\pm$ exchange irreducible background. As expected, the signal rate is rather low in comparison with the irreducible SM background. We thus do not expect this mode to be detectable. The modes explored in the previous subsections have much better reach, as we have demonstrated.

V. COMPARISON TO TECHNICOLOR STUDIES

Based on the AdS/CFT correspondence, the warped extra dimensional model is conjectured to be dual to purely

TABLE VIII. The cross sections (in fb) for the signal process $pp \to W' \to \ell\nu$ for case (i) and case (ii), and the SM background, with the cuts applied successively, for $M_{W'} = 2$ TeV.

2 TeV	Basic	$M_{\rm eff}$	M_T
Case (i)	0.04	0.024	0.012
Case (ii)	0.05	0.04	0.02
SM W	4×10^3	6.9	0.44

4D strong dynamics being involved in EWSB, such as technicolor or composite Higgs models. So, we expect similar signals for the two scenarios, and therefore it is useful to compare the extensive technicolor studies in the literature (see Ref. [47] for a review) with our current work on signals for electroweak KK gauge bosons in warped extra dimensions (including the neutral case studied earlier in Ref. [13]).

We begin with the details of this duality which will enable us to compare the signals that we studied to technicolor studies. The 5D model corresponds to a 4D theory with *two* sectors.[5] There is a sector which is strongly coupled, with the strength of the couplings in this sector remaining approximately constant over the Planck-weak hierarchy; i.e., it is a quasiconformal theory. Conformal invariance is broken at the TeV scale, resulting in a tower of composite (bound) states starting at ~TeV scale. The second sector consists of particles external to this conformal sector or elementary (as opposed to the composites of the strong sector above). However, these two sectors are not isolated; i.e., they do couple to each other. As a result, the elementary particles (external to the CFT sector) mix with the CFT composites and the mass eigenstates (physical states) are admixtures of the two sets of particles. These physical states correspond to the zero and KK modes of the 5D theory.

Furthermore, the location of a mode in the extra dimension is dual to the amount or degree of compositeness (in the sense of the elementary-composite mixture above) of the corresponding state in the 4D theory. Specifically, modes which are localized near the Planck (TeV) brane are interpreted as states which are mostly elementary (composite). Thus, the light SM fermions are mostly elementary, whereas the top quark, Higgs (including unphysical Higgs or longitudinal W/Z), and all KK's are mostly composites (the SM gauge bosons with a flat profile are in between in terms of compositeness). Roughly speaking, the KK tower of the 5D theory then corresponds to the tower of (massive) composites (''hadrons'') in the 4D theory. As discussed earlier, the coupling of a set of modes of the 5D theory is proportional to the overlap of the corresponding profiles in the extra dimension; i.e., it is large if all the modes of this set are localized near the TeV (or Planck) brane and small if some modes are localized near the Planck brane while others are localized near the TeV brane. In the dual 4D theory, the first situation corresponds to all the particles of the set being mostly composite (or mostly elementary), clearly resulting in a large coupling between these particles, while the second situation involves some particles which are mostly elementary and others which are mostly composites (thus accounting for the small coupling).

[5]See Ref. [29] for a two-site description of the 5D model (including the couplings to the heavy new particles) along these lines.

We now compare the nature of couplings and hence the decay channels in the warped extra dimensional model that we studied to the case of technicolor theories studied previously. First of all, the decays to *physical* Higgs bosons ($+ W/Z$) for the electroweak KK's that we studied are new compared to most technicolor studies. See, however, Ref. [48]. The reason is that in many technicolor theories, there would not be a light Higgs (see, however, Ref. [49]) since the basic idea of technicolor models is that the strong dynamics directly (spontaneously) breaks EW symmetry. Equivalently, WW scattering is unitarized by exchange of spin-1 bound states (techni-ρ's) instead of by a (light) Higgs. On the other hand, the warped extra dimensional model that we studied (with a light Higgs in the spectrum) is dual to composite Higgs models in 4D, i.e., where strong dynamics does not directly break EW symmetry. Rather, the strong dynamics produces a light composite Higgs which then acquires a vacuum expectation value in the low energy theory to break EW symmetry.

However, the decays of electroweak KK's to WZ or WW and production of KK's in vector boson fusion are (qualitatively) similar to those studied in the technicolor literature for the following reason. Recall that the decays of electroweak KK's to WZ and WW are dominated by *longitudinal* polarizations of the latter, with couplings which are enhanced relative to the SM. Since longitudinal W/Z are equivalent to unphysical Higgs, it is clear (based on the above discussion) that this coupling is dual to a self-coupling of three composites (i.e., techni-ρ with composite Goldstone bosons) in the 4D theory and thus is expected to be large. Clearly, such a coupling is a general characteristic of EWSB originating from strong dynamics and is present in all technicolor models studied in the literature. Of course, the details of these couplings at the quantitative level will be different in the 5D model than in the technicolor case (see Ref. [50] for a model-independent parametrization of couplings in composite Higgs models).

For the case of couplings of gauge KK's to fermions, it is convenient to consider two pieces or contributions in the formula for this coupling (see Table X) as follows. It can be shown that the piece $\propto 1/\xi$ comes from the overlap of profiles near the Planck or UV brane. This part of the coupling is dual to the SM fermion first coupling to the photon/W/Z (external to strong dynamics) which then mixes with the composite techni-ρ (analog of photon-ρ mixing in QCD). Clearly, this piece of the coupling is present in technicolor models studied in the literature as well and is flavor *universal*.

The contribution to the coupling of SM fermions to gauge KK's $\propto \xi$ originates from the overlap of profiles near the TeV or IR brane. In the 4D theory, this part of the coupling corresponds to a *direct* coupling of SM fermions to the techni-ρ, i.e., a coupling involving the *composite* component of the techni-ρ (as opposed to the coupling via techni-ρ's mixing with external gauge bo-

sons). Clearly such a contribution arises from (partial) compositeness of the SM fermions themselves and is of similar size to the fermions' coupling to the Higgs (which is another composite). Thus, this piece of the coupling is $\propto$ 4D or SM Yukawa coupling and is therefore flavor dependent.

This second contribution to the SM fermion coupling to KK's is absent in ''extended technicolor'' (ETC) [47], which is the mechanism used in traditional technicolor models to generate fermion masses (instead of partial compositeness of SM fermions as described above). In detail, in ETC the SM fermion masses originate from the coupling of *two* SM fermions to (a scalar operator of) strong dynamics such that there is no mixing of external fermions with composite fermions, unlike in the partial compositeness case which involves coupling of a *single* external fermion to (a fermionic operator of) strong dynamics. In any case, this piece of the coupling is irrelevant for production of gauge KK's via the DY process since that involves (dominantly) light fermions, whereas it is relevant for decays of gauge KK's into heavier SM fermions (top/bottom). Therefore, DY production of gauge KK's is (at least qualitatively) similar to that of techni-ρ's in technicolor, whereas decays to top quarks are different than in the simplest technicolor models with ETC.

In general, using the warped extra dimension framework has the advantage that we have a concrete, weakly coupled model so that we can ensure that we have a consistent set of couplings. In contrast, most technicolor studies simply used a parametrization for the various couplings rather than a well-defined model, although one could conceivably have such a model for these couplings by rescaling QCD data (assuming the strong dynamics is QCD-like).

Other differences between our analyses and earlier studies of technicolor are as follows. Most of the technicolor studies did not go beyond $\sim$2.5 TeV mass for the techni-ρ's, although the heavier end of the mass range was preferred by constraints from EWPT (specifically, the S parameter), while we have considered signals for electroweak KK's up to 3 TeV. Finally, the semileptonic decay of the WW or WZ has not been studied in detail in the technicolor context, especially the use of the jet-mass cut to discriminate a W/Z jet from a QCD jet.

VI. DISCUSSION AND CONCLUSIONS

In the past few years, it has been shown that the framework of a warped extra dimension with SM fields in the bulk can address many of the puzzles of nature. Thus, this framework is a very attractive extension of the SM (perhaps as compelling as SUSY). As the LHC has started, it is very crucial to study in this framework robust signals from the *direct* production at the LHC of the new particles, namely, the KK excitations of the SM. Over the last year or so, such analyses have been performed for the KK gluon, graviton, Z, and some fermions. Here, we continue this program with a study of the *charged* electroweak KK gauge bosons (W'), thus completing the study of spin-1 states in this framework. We summarize in Table IX the LHC reach for the two t_R cases discussed in Sec. II C with representations shown in Eq. (B2), extracting from the detailed analysis we presented in Sec. IV the best channel for each of the W' decay modes. We give the luminosity and resulting significance for the mass shown. We find that we can get a sensitivity of 2(3) TeV masses with an integrated luminosity of about 100(300) fb^{-1}, which, although slightly better, is comparable to the KK Z reach obtained in Ref. [13].

It is instructive to compare our analysis to the previous ones, starting with various spin-1 states, in order to illustrate the complementarity of the various studies. The KK gluon has the largest cross section in this framework, but it decays mostly into $t\bar{t}$ which results in exclusively jetty final states, even if the W from the top decays to leptons (due to the high degree of collimation of decay products of the top quarks). On the other hand, KK W decays into WZ can result in clean, purely leptonic and fully reconstructible final states, albeit with a small BR, which in the end does not result in the reach being larger in this channel.[6] In contrast, KK Z decays into WW can also result in purely leptonic final states, but the invariant mass is not reconstructible in this case. The semileptonic analogues of these decays for KK W/Z (i.e., one W/Z decaying leptonically and the other hadronically) are on a similar footing to the KK gluon in terms of cleanness since the detection of the highly collimated hadronically decaying W/Z requires discriminating it from the QCD-jet background (just like for highly collimated top quarks from decays of the KK gluon): in our analysis a jet-mass cut was used for this purpose. Finally, KK Z decays to top pairs are swamped by KK-gluon background,[7] but KK W decays to $t\bar{b}$ do not have this problem if the background from the KK gluon to $t\bar{t}$ with one highly boosted top faking a bottom can be reduced, for example, again by using jet mass as we did here.

[6]In more detail, the ability to reconstruct the WZ invariant mass makes the S/B larger, but the effect is diluted a bit when we consider $S/\sqrt{B}$. The effect of a smaller BR of WZ vs WW to leptons cancels in S/B, but still tends to reduce $S/\sqrt{B}$. So, the net result is a significantly larger S/B for the former case, but $S/\sqrt{B}$ is not larger by as much. Another issue is that the KK W can decay into one KK and one zero-mode fermion in the setups that we considered (with decays to *two* light KK fermions being kinematically forbidden in the cases that we study). The presence of this channel dilutes the BR to WZ for the KK W. Such a decay channel is suppressed for the KK Z since the light KK fermion comes from a *different* 5D fermion field than the zero-mode fermion, and thus $U(1)$ gauge bosons [including $U(1)$ subgroups of non-Abelian gauge multiplets] such as the Z cannot couple these two fermions.

[7]Assuming a small mass splitting between the KK Z and the KK gluon as in the simplest models with no brane-localized kinetic terms for bulk gauge fields.

TABLE IX. Summary of the best channel for each of the W' decay modes, giving the luminosity and significance (S_σ) for the mass shown, in the two t_R coupling scenarios of cases (i) and (ii). The significance is computed as $S_\sigma = S/\sqrt{B}$, but when the number of events is small, we use Poisson statistics and quote an equivalent Gaussian significance. For the tb channel the numbers without (and with) the reducible $t\bar{t}$ background are shown.

Case (i): Channel	$M_{W'}$ (TeV)	$\mathcal{L}$ (fb^{-1})	S/B	S_σ
$tb \to \ell\nu b\bar{b}$	3	300	5.8 (0.9)	4.5 (2.2)
$ZW \to \ell\ell\ell\nu$	3	1000	6	4.3
$m_h = 120$: $Wh \to \ell\nu b\bar{b}$	3	300	1	2.75
$m_h = 150$: $Wh \to (jj)\ell\nu(jj)$	3	300	2	4

Case (ii): Channel	$M_{W'}$ (TeV)	$\mathcal{L}$ (fb^{-1})	S/B	S_σ
$tb \to \ell\nu b\bar{b}$	2	1000	0.4 (0.2)	3.4 (2.5)
$ZW \to \ell\ell\ell\nu$	3	1000	10	6
$m_h = 120$: $Wh \to \ell\nu b\bar{b}$	3	300	2.4	6.2
$m_h = 150$: $Wh \to (jj)\ell\nu(jj)$	3	300	4	8

TABLE X. Values of $\psi\psi W'$ overlap integrals: Case (i), $t_R \to (1, 1)$, $c_{Q_L^3} = 0$, and $c_{t_R} = 0.4$ (upper table), and case (ii), $t_R \to (1, 3)$, $c_{Q_L^3} = 0.4$, and $c_{t_R} = 0$ (lower table). All the other c's >0.5. We take $\xi = \sqrt{k\pi r_c} = 5.83$. All SM fermions have $(++)$ BC, exotic beyond-the-standard-model fermions have $(-+)$, W_{L_1} has $(++)$, and W_{R_1} has $(-+)$ BC.

$c_{Q_L^3} = 0$, $c_{t_R} = 0.4$	Q_L^3	t_R	Other fermions
$I^{++}_{++,++}$	$-\frac{1.13}{\xi} + 0.7\xi \approx 3.9$	$-\frac{1.13}{\xi} + 0.2\xi \approx 1$	$-\frac{1.13}{\xi} \approx -0.2$
$I^{++}_{-+,-+}$	ξ	ξ	$\cdots$
$I^{-+}_{++,-+}$	$0.8\xi \approx 4.6$	$0.4\xi \approx 2.3$	≈ 0

$c_{Q_L^3} = 0.4$, $c_{t_R} = 0$	Q_L^3	t_R	Other fermions
$I^{++}_{++,++}$	$-\frac{1.13}{\xi} + 0.2\xi \approx 1$	$-\frac{1.13}{\xi} + 0.7\xi \approx 3.9$	$-\frac{1.13}{\xi} \approx -0.2$
$I^{++}_{-+,-+}$	ξ	ξ	$\cdots$
$I^{-+}_{++,-+}$	$0.4\xi \approx 2.3$	$0.8\xi \approx 4.6$	≈ 0

We reiterate that further development of techniques for detecting highly boosted W/Z jets and similarly vetoing a highly boosted top faking a bottom can improve the reach for charged (and also neutral) EW states. Another feature we would like to mention is that there are two extreme possibilities for the profiles of top/bottom quarks which are relevant for the KK W search, namely, where the right-handed or left-handed top is localized near the so-called TeV brane in the extra dimension (while the other chirality has a close-to-flat profile)—the point is that either t_R or t_L must be localized near the TeV brane in order to obtain the large top mass. The first possibility is favored by flavor precision tests, whereas EW precision tests have a milder preference for the second. Note that the KK modes are also localized near the TeV brane. Hence, the coupling of the KK W (and hence the BR) to left-handed t (and $\bar{b}$)[8] is suppressed or enhanced in the two cases and thus vice versa for BR of the other channels with significant couplings to the KK W, i.e., WZ and Wh, making the two search channels (i.e., $t\bar{b}$ and WZ/h) complementary in the case of the KK W. These two choices for top profiles make less of a difference for the KK Z search since the KK Z always has substantial BR to decay into SM top pairs (of whichever chirality—LH or RH—is localized near the TeV brane).

For a complete perspective of this research program, we now comment on the other spin states. The spin-2 KK graviton is typically heavier than the spin-1 states and thus has an even smaller production cross section. Its decays to $t\bar{t}$ are *not* likely to be swamped by those of the KK gluon due to the different mass, but one faces the (even more difficult) challenge of identifying highly boosted top quarks. Decays to ZZ followed by leptons are possibly the cleanest and can moreover be fully reconstructed, but suffer from a very small BR. In contrast, decays to WW cannot be reconstructed in the fully leptonic case (just like in the case of KK Z), and challenges for the semileptonic case are similar to KK W/Z from QCD background.

As far as KK fermions are concerned, the masses of the KK excitations of top/bottom (and their other gauge-group partners) in some models (where the 5D gauge symmetry is

[8]The decays of KK W to t_R and b_R are usually suppressed since b_R is localized near the Planck brane.

extended beyond that in the SM) can be (much) smaller than gauge KK modes, enhancing the prospect for their discovery. In fact, the other heavier (spin-1 or 2) KK modes can decay into these light KK fermions, resulting in perhaps more distinctive final states for the heavy KK's than the pairs of W/Z or top quarks that have been studied so far—for a recent such study for the KK gluon, see Ref. [11]. A few studies of signals for the heavier KK fermions and of the radion have also been done. We leave more detailed studies of heavier KK fermions and radion (as well as the rather model-dependent decays of a heavier KK $Z/W/$graviton into lighter KK's or radion) for future work.

We would like to emphasize that the signals we studied in this paper (and the previous one on neutral gauge bosons) might actually be valid for a wider class of nonsupersymmetric models of EWSB. For example, based on AdS/CFT correspondence discussed in Sec. V, it is clear that any kind of 4D strong dynamics involved in EWSB will (in general) share many of the features of the 5D model. Also, the parameter space of little Higgs models which satisfies EWPT corresponds to the W', Z' being weakly coupled to light fermions and strongly coupled to Higgs (including longitudinal W/Z) [51], just like in the 5D models we studied here. Moreover, some UV completions of little Higgs involve 4D strong dynamics which might have a dual warped extra dimensional description. Thus, little Higgs models and EWSB models with strong dynamics are likely to have LHC signals similar to the ones we have studied. Note, however, that the flavor structure of the warped extra dimension is different than in traditional technicolor models so that the decays of KK W/Z to top/bottom are new features. We would also like to point out that the jet-mass cut for semileptonic decays of WZ or WW from the decay of heavy W/Z has not been studied in detail in these other contexts (technicolor or little Higgs).

In more generality, the point is that there is a class of nonsupersymmetric extensions of the SM without a symmetry (analogous to R parity in SUSY) which allow tree-level exchange of new particles to contribute to (purely) SM operators, resulting in strong constraints from precision tests, typically a few TeV mass for the new particles. Moreover, in many such models, the top/bottom quark and Higgs, including the longitudinal W/Z, couple strongly to the new particles since all these particles are closely associated with EWSB. On the other hand, the coupling of the new states to light fermions is typically weak, in part based on considerations of flavor and EW precision tests. Thus, a large class of nonsupersymmetric models faces challenges similar to the warped extra dimension framework that we studied here; namely, production of the new states tends to be suppressed and decays are mostly to top quarks/W/Z, which are highly boosted. In summary, the techniques we developed in this paper might be useful for obtaining signals for a wider class of models, beyond warped extra dimensions.

ACKNOWLEDGMENTS

We would like to thank H. Davoudiasl, D. E. Kaplan, W. Kilgore, F. Paige, G. Perez, Z. Si, C. Sturm, M. Strassler, and R. Sundrum for discussions; A. Belyaev for help with CALCHEP; and S. Mrenna and P. Skands for help with PYTHIA. K. A. is supported in part by NSF Grant No. PHY-0652363. S. G. and A. S. are supported in part by the DOE Grant No. DE-AC02-98CH10886 (BNL). T. H and G.-Y. H. are supported in part by DOE Grant No. DE-FG02-95ER40896 and in part by the Wisconsin Alumni Research Foundation, and G.-Y. H. is also supported by DOE Grant No. DE-FG02-91ER40674 and by the U.C. Davis HEFTI program.

APPENDIX A: MIXING ANGLES

The electroweak gauge group in the bulk is $SU(2)_L \times SU(2)_R \times U(1)_X$, with the hypercharge being a linear combination of $U(1)_R$ and $U(1)_X$. The extra $SU(2)_R$ (relative to the SM) ensures suppression of contribution to the EWPT (specifically, an observable called the T parameter). Hence, we obtain two charged 5D fields—one from each $SU(2)$ group in the bulk—denoted as $W_L^{\pm}$ and $W_R^{\pm}$. In addition, there are three neutral 5D electroweak gauge bosons denoted as W_L^3, W_R^3, and X whose theory and LHC phenomenology was explored in Ref. [13]. These bulk gauge fields can be expanded as a tower of KK states. As explained in detail in Ref. [13], the $SU(2)_R \otimes U(1)_X \to U(1)_Y$ symmetry breaking by boundary conditions (BC) leaves a zero mode in one combination of (W_R^3, X) (the hypercharge gauge boson $B^{(0)}$) while rendering the orthogonal combination (denoted by Z_X) (and $W_R^{\pm}$) without a zero mode. Also, $SU(2)_L \otimes U(1)_Y \to U(1)_{EM}$ symmetry breaking by the Higgs vacuum expectation value leaves one combination of (W_L^3, B) zero modes massless (the photon $A^{(0)}$), while making the orthogonal combination ($Z^{(0)}$) (and the $W_L^{\pm(0)}$) massive. In addition to the above zero modes, in each of these charged and neutral towers of states, we will restrict to the first KK modes only and denote the charged ones by W_{L_1} and W_{R_1}, and the neutral ones by A_1, Z_1, and Z_{X1}. EWSB also mixes these first KK modes with each other (and with $Z^{(0)}$, $W_L^{\pm(0)}$) and the resulting heavy mass eigenstates are denoted by the charged $\tilde{W}_{L_1}$, $\tilde{W}_{R_1}$, and the neutral $\tilde{A}_1$, $\tilde{Z}_1$, and $\tilde{Z}_{X_1}$ states.

Here we collect from Ref. [13], expressions for the mixing angles mentioned above: for more details, see this reference. These mixing effects can be conveniently expressed in terms of the following parameters [with $s \equiv \sin()$ and $c \equiv \cos()$]

$$e = \frac{g_L g'}{\sqrt{g'^2 + g_L^2}}, \qquad g_Z = g_L / c_W, \tag{A1}$$

$$s_W = \frac{g'}{\sqrt{g'^2 + g_L^2}}, \qquad c_W = \sqrt{1 - s_W^2}, \tag{A2}$$

$$g' = \frac{g_X g_R}{\sqrt{g_R^2 + g_X^2}}, \qquad g_{Z'} = g_R/c', \tag{A3}$$

$$s' = \frac{g_X}{\sqrt{g_R^2 + g_X^2}}, \qquad c' = \sqrt{1 - s'^2}. \tag{A4}$$

The first two relations above (involving mixing of $B^{(0)}$ and $W_L^{3(0)}$) are just the usual SM ones. The last two relations above are the analogs of the first two, but involve mixing of W_R^3 and X instead (with g_X denoting the coupling of the ''would-be'' X zero mode). For our numerical study, we assume $g_L = g_R$ throughout, which is motivated by custodial symmetry protection for $Zb\bar{b}$. For this case, we have $s' = 0.55$, $c' = 0.84$.

As explained in Appendixes A and B of Ref. [13], EWSB induces a mixing between $Z^{(0)} \leftrightarrow Z_1$ (with mixing angle θ_{01}) and $Z^{(0)} \leftrightarrow Z_{X1}$ (with mixing angle θ_{01X}). To leading order in $M_Z/M_{Z'}$, these mixing angles are given by

$$\sin\theta_{01} \approx \left(\frac{M_Z}{M_{Z_1}}\right)^2 \sqrt{k\pi r_c}, \tag{A5}$$

$$\sin\theta_{01X} \approx -\left(\frac{M_Z}{M_{Z_{X1}}}\right)^2 \left(\frac{g_{Z'}}{g_Z}\right) c'^2 \sqrt{k\pi r_c}. \tag{A6}$$

For example, for $M_{Z'} = 2$ TeV, $s_{01} = 0.013$ and $s_{01X} = -0.01$.

EWSB similarly induces mixing in the charged $W^\pm$ sector, i.e. mixing between $W \leftrightarrow W'$, with the mixing angle given by

$$\sin\theta_{0L} \approx \left(\frac{M_W}{M_{W_{L_1}}}\right)^2 \sqrt{k\pi r_c}, \tag{A7}$$

$$\sin\theta_{0R} \approx -\left(\frac{M_W}{M_{W_{R_1}}}\right)^2 \left(\frac{g_R}{g_L}\right) \sqrt{k\pi r_c}. \tag{A8}$$

For example, for $M_{Z'} = 2$ TeV, $s_{0L} \approx 0.01$ and $s_{0R} \approx -0.01$.

EWSB also induces $Z_1 \leftrightarrow Z_{X1}$ mixing, with the mixing angle given by

$$\tan 2\theta_1 = \frac{-2M_Z^2 (g_{Z'}/g_Z) c'^2 k\pi r_c}{(M_{Z_{X1}}^2 - M_{Z_1}^2) + M_Z^2((g_{Z'}/g_Z)^2 c'^4 - 1) k\pi r_c}. \tag{A9}$$

For example, for $M_{Z_1} = 2000$; $M_{Z_{X1}} = 1962$ GeV, this implies that $s_1 = 0.48$, $c_1 = 0.88$. After this mixing, we will refer to the mass eigenstates as $\tilde{Z}_1$ and $\tilde{Z}_{X1}$.

EWSB similarly induces $W_{L_1} \leftrightarrow W_{R_1}$, with the mixing angle given by

$$\tan 2\theta_1^c = \frac{-2M_W^2 (g_R/g_L) k\pi r_c}{(M_{W_{R_1}}^2 - M_{W_{L_1}}^2) + M_W^2((g_R/g_L)^2 - 1) k\pi r_c}. \tag{A10}$$

For example, for $M_{W_{L_1}} = 2000$; $M_{W_{R_1}} = 1962$ GeV, this implies that $s_1^c = 0.6$, $c_1^c = 0.8$. After this mixing, we will refer to the mass eigenstates as $\tilde{W}_{L_1}$ and $\tilde{W}_{R_1}$, and for notational ease they were denoted by W_L' and W_R', respectively, in the main text.

APPENDIX B: COUPLINGS OF W'

We work in the approximation $(k\pi r_c) m_W^2/M_{KK}^2 \ll 1$. We focus mainly on the fermion representation with the custodial symmetry protecting $Zb\bar{b}$.

1. W' coupling to fermions

We show below the fermion representations under $SU(2)_L \otimes SU(2)_R \otimes U(1)_X$, denoted as $(L, R)_X$. We take the left-handed quarks of the first and second generations, and the left-handed leptons to be doublets under $SU(2)_L$. This specifies the interaction of these fields with W_{L_1}. The W_{R_1} couplings to first and second generation quarks, right-handed bottom quark, and leptons are negligibly small since the W_{R_1} profile is suppressed near the Planck brane where these fermion fields are peaked. To have the custodial symmetry protection of the $Zb\bar{b}$ coupling [37], we take the third generation left-handed quarks to be in the representation

$$Q_L^3 = \begin{pmatrix} q_L^3 & q_L'^3 \end{pmatrix} = \begin{pmatrix} t_L & \chi_L \\ b_L & T_L \end{pmatrix} \rightarrow (2, 2)_{2/3}, \tag{B1}$$

where χ_L, T_L are taken to have $(-+)$ BC with no zero modes,[9] with $-$ denoting Dirichlet BC and $+$ denoting Neumann BC. We have $Q(\chi_L) = 5/3$ and $Q(T_L) = 2/3$. To accommodate the large top and bottom mass difference, we assume that t_R and b_R do not belong to the same $SU(2)_R$ multiplet. We consider two cases for the t_R representations,

$$\text{Case (i): } t_R \rightarrow (1, 1)_{2/3},$$

$$\text{Case(ii): } t_R \rightarrow (1, 3)_{2/3} \oplus (3, 1)_{2/3} = \begin{pmatrix} \chi_R'' \\ t_R \\ B_R'' \end{pmatrix} \oplus \begin{pmatrix} \chi_R''' \\ T_R''' \\ B_R''' \end{pmatrix}, \tag{B2}$$

where the non-SM fermions have $(-+)$ BC with no zero modes, and the fermions in the (3, 1) representation are not discussed further in our work here since the W' decay to a pair of them is kinematically forbidden. For case (i), $t_R \rightarrow (1, 1)$, the EWPT are better satisfied [38] for $c_{Q_L^3} = 0$ and $c_{t_R} = 0.4$, i.e., Q_L^3 peaked closer to the TeV brane, while for case (ii), $t_R \rightarrow (1, 3)$, for $c_{Q_L^3} = 0.4$ and $c_{t_R} = 0$, i.e., c_{t_R}

[9] All SM fermions have $(++)$ BC since they are zero modes.

peaked closer to the TeV brane. After including the charges and the overlap integrals, the largest effective coupling of third generation fermions to gauge KK modes in case (i) would be to Q_L^3, being larger than that in case (ii), which would be to t_R. Consequently, while on the one hand, FCNC's induced by coupling of gauge KK to b_L would be larger in case (i) and hence more problematic for the simplest constructions, on the other hand collider signals in the $t\bar{b}$ channel would be larger compared to case (ii).

The fermion couplings to W' depend on various mixing angles summarized in Appendix A. The couplings also depend on the overlap of the profiles, which we give next. We note that W_{L_1} has $(++)$ while W_{R_1} has $(-+)$ BC. The overlap integrals of a W' with two fermions are given in Table X. We represent by $\mathcal{I}^{xx}_{yy,zz}$ the overlap integral of the W' having xx BC with two fermion fields, one with yy and the other with zz BC. For instance, $\mathcal{I}^{++}_{++,++}$ is the overlap integral of the W_{L_1} with two fermions, both with $(++)$ BC, and $\mathcal{I}^{++}_{++,-+}$ the overlap integral of the W_{L_1} with one fermions with $(++)$ BC and the other with $(-+)$ BC. Similarly, $\mathcal{I}^{-+}_{yy,zz}$ represents the overlap integral of the W_{R_1} with two fermions. Because of the orbifold Z_2 symmetry, we have $I^{++}_{++,-+} = 0$ etc., and we show only the nonzero ones in the table.

We note that the mass of the $(-+)$ fermion is lighter than $M_{\tilde{W}_{L_1}}$ for $c < 1/2$. In particular, for $c = 0.4$ it is about $0.9M_{\tilde{W}_{L_1}}$, and for $c = 0$ it is about $0.6M_{\tilde{W}_{L_1}}$. The first KK excitations of the $(++)$ fermions are typically heavier than $M_{\tilde{W}_{L_1}}$ (being equal at $c = 1/2$).

The W' coupling (Feynman rule) to fermions is given by

$$\bar{u}_L d_L\{\tilde{W}^+_{L_1}, \tilde{W}^+_{R_1}\}\colon\ i\frac{g_L}{\sqrt{2}}\{c_1^c, s_1^c\}\mathcal{I}^{++}_{u_L d_L}, \tag{B3}$$

where u_L (d_L) denotes first and second generation up- (down-) type fermions. The third generation left-handed fermion couplings are given by

$$\begin{aligned}
&\bar{t}_L b_L\{\tilde{W}^+_{L_1}, \tilde{W}^+_{R_1}\}\colon\ i\frac{g_L}{\sqrt{2}}\{c_1^c, s_1^c\}\mathcal{I}^{++}_{t_L b_L},\\
&\bar{\chi}_L T_L\{\tilde{W}^+_{L_1}, \tilde{W}^+_{R_1}\}\colon\ i\frac{g_L}{\sqrt{2}}\{c_1^c, s_1^c\}\mathcal{I}^{++}_{\chi_L T_L},\\
&\bar{\chi}_L t_L\{\tilde{W}^+_{L_1}, \tilde{W}^+_{R_1}\}\colon\ i\frac{g_R}{\sqrt{2}}\{s_1^c, -c_1^c\}\mathcal{I}^{-+}_{\chi_L t_L},\\
&\bar{T}_L b_L\{\tilde{W}^+_{L_1}, \tilde{W}^+_{R_1}\}\colon\ i\frac{g_R}{\sqrt{2}}\{s_1^c, -c_1^c\}\mathcal{I}^{-+}_{T_L b_L}.
\end{aligned} \tag{B4}$$

For case (i), $t_R \to (1, 1)$, it does not interact with the W', as already mentioned. For case (ii), $t_R \to (1, 3)$, its interaction with the W' is given as

$$\begin{aligned}
&\bar{\chi}''_R t_R\{\tilde{W}^+_{L_1}, \tilde{W}^+_{R_1}\}\colon\ -i\frac{g_R}{2}\{-s_1^c, c_1^c\}\mathcal{I}^{-+}_{\chi''_R t_R},\\
&\bar{t}_R B''_R\{\tilde{W}^+_{L_1}, \tilde{W}^+_{R_1}\}\colon\ i\frac{g_R}{2}\{-s_1^c, c_1^c\}\mathcal{I}^{-+}_{t_R B''_R}.
\end{aligned} \tag{B5}$$

2. W' coupling to two SM gauge bosons

In order to derive the triple gauge-boson coupling, we start with the KK basis Lagrangian terms (keeping in mind $W_R^{\pm(0)} \equiv 0$)

$$\begin{aligned}
\mathcal{L} \supset\ &-g_L W_L^{3(0)} W_L^{+(0)} W_L^{-(0)} - g_L W_L^{3(1)} W_L^{+(1)} W_L^{-(0)}\\
&- g_L W_L^{3(0)} W_L^{+(1)} W_L^{-(1)} - g_R W_R^{3(0)} W_R^{+(1)} W_R^{-(1)}.
\end{aligned} \tag{B6}$$

Writing this in the mass eigenstate basis after EWSB results in the triple gauge-boson couplings (Feynman rules). The $AW'^{\pm}W^{\mp}$ coupling is zero. The Z couplings (Feynman rules) are given by

$$\begin{aligned}
&Z\tilde{W}^+_{L_1} W^-\colon\ -ig_L c_W\left[-s_{0R}s_1^c\left(\frac{g_R}{g_L}\frac{s_W}{c_W}s' + 1\right) - s_{01}c_1^c\right],\\
&Z\tilde{W}^+_{R_1} W^-\colon\ -ig_L c_W\left[s_{0R}c_1^c\left(\frac{g_R}{g_L}\frac{s_W}{c_W}s' + 1\right) - s_{01}s_1^c\right],
\end{aligned} \tag{B7}$$

and for comparison, we note that the SM triple gauge-boson coupling is given as $\{A, Z\}W^+W^-\colon -ig_L\{s_W, c_W\}$.

3. W' coupling to the W and Higgs

Starting from Eq. (44) of Ref. [13], we obtain the couplings to the Higgs by making the substitution $v \to (v + h)$, which results in the couplings (Feynman rules)

$$\begin{aligned}
&\{\tilde{W}^+_{L_1}, \tilde{W}^+_{R_1}\}W^- h\colon i\frac{2m_W^2}{v}\sqrt{k\pi r_c}\left\{\left(c_1^c + \frac{g_R}{g_L}s_1^c\right), \left(s_1^c - \frac{g_R}{g_L}c_1^c\right)\right\},\\
&\{\tilde{W}^+_{L_1}, \tilde{W}^+_{R_1}\}W^- hh\colon i\frac{2m_W^2}{v^2}\sqrt{k\pi r_c}\left\{\left(c_1^c + \frac{g_R}{g_L}s_1^c\right), \left(s_1^c - \frac{g_R}{g_L}c_1^c\right)\right\},
\end{aligned} \tag{B8}$$

where the hh couplings include a symmetry factor of 2.

[1] L. Randall and R. Sundrum, Phys. Rev. Lett. **83**, 3370 (1999).

[2] H. Davoudiasl, J. L. Hewett, and T. G. Rizzo, Phys. Lett. B **473**, 43 (2000); A. Pomarol, Phys. Lett. B **486**, 153

(2000); S. Chang, J. Hisano, H. Nakano, N. Okada, and M. Yamaguchi, Phys. Rev. D **62**, 084025 (2000).
[3] Y. Grossman and M. Neubert, Phys. Lett. B **474**, 361 (2000).
[4] T. Gherghetta and A. Pomarol, Nucl. Phys. **B586**, 141 (2000).
[5] K. Agashe, R. Contino, and R. Sundrum, Phys. Rev. Lett. **95**, 171804 (2005).
[6] K. Agashe and G. Servant, Phys. Rev. Lett. **93**, 231805 (2004); J. Cosmol. Astropart. Phys. 02 (2005) 002.
[7] T. G. Rizzo, J. High Energy Phys. 06 (2002) 056; C. Csaki, J. Hubisz, and S. J. Lee, Phys. Rev. D **76**, 125015 (2007); M. Toharia, Phys. Rev. D **79**, 015009 (2009).
[8] K. Agashe, A. Belyaev, T. Krupovnickas, G. Perez, and J. Virzi, Phys. Rev. D **77**, 015003 (2008).
[9] B. Lillie, L. Randall, and L. T. Wang, J. High Energy Phys. 09 (2007) 074.
[10] M. Guchait, F. Mahmoudi, and K. Sridhar, J. High Energy Phys. 05 (2007) 103; B. Lillie, J. Shu, and T. M. P. Tait, Phys. Rev. D **76**, 115016 (2007); A. Djouadi, G. Moreau, and R. K. Singh, Nucl. Phys. **B797**, 1 (2008); M. Guchait, F. Mahmoudi, and K. Sridhar, Phys. Lett. B **666**, 347 (2008).
[11] M. Carena, A. D. Medina, B. Panes, N. R. Shah, and C. E. M. Wagner, Phys. Rev. D **77**, 076003 (2008).
[12] A. L. Fitzpatrick, J. Kaplan, L. Randall, and L. T. Wang, J. High Energy Phys. 09 (2007) 013; K. Agashe, H. Davoudiasl, G. Perez, and A. Soni, Phys. Rev. D **76**, 036006 (2007); O. Antipin, D. Atwood, and A. Soni, Phys. Lett. B **666**, 155 (2008); O. Antipin and A. Soni, J. High Energy Phys. 10 (2008) 018.
[13] K. Agashe *et al.*, Phys. Rev. D **76**, 115015 (2007).
[14] H. Davoudiasl, T. G. Rizzo, and A. Soni, Phys. Rev. D **77**, 036001 (2008).
[15] C. Dennis, M. Karagoz Unel, G. Servant, and J. Tseng, arXiv:hep-ph/0701158; R. Contino and G. Servant, J. High Energy Phys. 06 (2008) 026.
[16] H. Davoudiasl, J. L. Hewett, and T. G. Rizzo, Phys. Rev. Lett. **84**, 2080 (2000); Phys. Rev. D **63**, 075004 (2001); S. C. Park, H. S. Song, and J. H. Song, Phys. Rev. D **65**, 075008 (2002); H. Davoudiasl and T. G. Rizzo, Phys. Lett. B **512**, 100 (2001); H. Davoudiasl, J. L. Hewett, B. Lillie, and T. G. Rizzo, Phys. Rev. D **70**, 015006 (2004); A. Birkedal, K. Matchev, and M. Perelstein, Phys. Rev. Lett. **94**, 191803 (2005); F. Ledroit, G. Moreau, and J. Morel, J. High Energy Phys. 09 (2007) 071; A. Djouadi and G. Moreau, Phys. Lett. B **660**, 67 (2008); M. Piai, arXiv:0704.2205.
[17] R. Contino, Y. Nomura, and A. Pomarol, Nucl. Phys. **B671**, 148 (2003).
[18] W. D. Goldberger and M. B. Wise, Phys. Rev. Lett. **83**, 4922 (1999); J. Garriga and A. Pomarol, Phys. Lett. B **560**, 91 (2003).
[19] J. M. Maldacena, Adv. Theor. Math. Phys.. **2**, 231 (1998); Int. J. Theor. Phys. **38**, 1113 (1999); S. S. Gubser, I. R. Klebanov, and A. M. Polyakov, Phys. Lett. B **428**, 105 (1998); E. Witten, Adv. Theor. Math. Phys. **2**, 253 (1998).
[20] N. Arkani-Hamed, M. Porrati, and L. Randall, J. High Energy Phys. 08 (2001) 017; R. Rattazzi and A. Zaffaroni, J. High Energy Phys. 04 (2001) 021.
[21] S. J. Huber and Q. Shafi, Phys. Lett. B **498**, 256 (2001).
[22] K. Agashe, G. Perez, and A. Soni, Phys. Rev. D **71**, 016002 (2005).
[23] C. Csaki, A. Falkowski, and A. Weiler, J. High Energy Phys. 09 (2008) 008; M. Blanke, A. J. Buras, B. Duling, S. Gori, and A. Weiler, J. High Energy Phys. 03 (2009) 001.
[24] A. L. Fitzpatrick, G. Perez, and L. Randall, Phys. Rev. Lett. **100**, 171604 (2008).
[25] S. Davidson, G. Isidori, and S. Uhlig, Phys. Lett. B **663**, 73 (2008).
[26] H. Davoudiasl, B. Lillie, and T. G. Rizzo, J. High Energy Phys. 08 (2006) 042; M. Piai, arXiv:hep-ph/0608241; G. Cacciapaglia, C. Csaki, G. Marandella, and J. Terning, J. High Energy Phys. 02 (2007) 036; J. Hirn and V. Sanz, J. High Energy Phys. 03 (2007) 100; C. D. Carone, J. Erlich, and J. A. Tan, Phys. Rev. D **75**, 075005 (2007).
[27] P. McGuirk, G. Shiu, and K. M. Zurek, J. High Energy Phys. 03 (2008) 012; G. Shiu, B. Underwood, K. M. Zurek, and D. G. E. Walker, Phys. Rev. Lett. **100**, 031601 (2008); A. Falkowski and M. Perez-Victoria, J. High Energy Phys. 12 (2008) 107; B. Batell, T. Gherghetta, and D. Sword, Phys. Rev. D **78**, 116011 (2008).
[28] M. Carena, E. Ponton, T. M. P. Tait, and C. E. M. Wagner, Phys. Rev. D **67**, 096006 (2003); H. Davoudiasl, J. L. Hewett, and T. G. Rizzo, Phys. Rev. D **68**, 045002 (2003); M. S. Carena, A. Delgado, E. Ponton, T. M. P. Tait, and C. E. M. Wagner, Phys. Rev. D **68**, 035010 (2003); **71**, 015010 (2005).
[29] R. Contino, T. Kramer, M. Son, and R. Sundrum, J. High Energy Phys. 05 (2007) 074.
[30] K. Agashe, A. Azatov, and L. Zhu, Phys. Rev. D **79**, 056006 (2009).
[31] G. Cacciapaglia, C. Csaki, J. Galloway, G. Marandella, J. Terning, and A. Weiler, J. High Energy Phys. 04 (2008) 006; M. C. Chen and H. B. Yu, Phys. Lett. B **672**, 253 (2009); G. Perez and L. Randall, J. High Energy Phys. 01 (2009) 077; C. Csaki, C. Delaunay, C. Grojean, and Y. Grossman, J. High Energy Phys. 10 (2008) 055; J. Santiago, J. High Energy Phys. 12 (2008) 046; C. Csaki, A. Falkowski, and A. Weiler, Phys. Rev. D **80**, 016001 (2009); C. Csaki, Y. Grossman, G. Perez, Z. Surujon, and A. Weiler (unpublished).
[32] H. Davoudiasl, G. Perez, and A. Soni, Phys. Lett. B **665**, 67 (2008).
[33] P. M. Aquino, G. Burdman, and O. J. P. Eboli, Phys. Rev. Lett. **98**, 131601 (2007).
[34] For studies with $\sim$10 TeV KK masses, see S. J. Huber, Nucl. Phys. **B666**, 269 (2003); S. Khalil and R. Mohapatra, Nucl. Phys. **B695**, 313 (2004).
[35] G. Burdman, Phys. Lett. B **590**, 86 (2004); K. Agashe, G. Perez, and A. Soni, Phys. Rev. Lett. **93**, 201804 (2004); G. Moreau and J. I. Silva-Marcos, J. High Energy Phys. 03 (2006) 090; K. Agashe, A. E. Blechman, and F. Petriello, Phys. Rev. D **74**, 053011 (2006); K. Agashe, G. Perez, and A. Soni, Phys. Rev. D **75**, 015002 (2007); S. Chang, C. S. Kim, and J. Song, J. High Energy Phys. 02 (2007) 087; Phys. Rev. D **77**, 075001 (2008); W. F. Chang, J. N. Ng, and J. M. S. Wu, Phys. Rev. D **78**, 096003 (2008); **79**, 056007 (2009).
[36] K. Agashe, A. Delgado, M. J. May, and R. Sundrum, J. High Energy Phys. 08 (2003) 050.

[37] K. Agashe, R. Contino, L. Da Rold, and A. Pomarol, Phys. Lett. B **641**, 62 (2006).

[38] K. Agashe, R. Contino, and A. Pomarol, Nucl. Phys. **B719**, 165 (2005); K. Agashe and R. Contino, Nucl. Phys. **B742**, 59 (2006); M. Carena, E. Ponton, J. Santiago, and C. E. M. Wagner, Nucl. Phys. **B759**, 202 (2006); Phys. Rev. D **76**, 035006 (2007); R. Contino, L. Da Rold, and A. Pomarol, Phys. Rev. D **75**, 055014 (2007); A. D. Medina, N. R. Shah, and C. E. M. Wagner, Phys. Rev. D **76**, 095010 (2007); C. Bouchart and G. Moreau, Nucl. Phys. **B810**, 66 (2009); S. Casagrande, F. Goertz, U. Haisch, M. Neubert, and T. Pfoh, J. High Energy Phys. 10 (2008) 094.

[39] V. Barger, T. Han, and D. G. E. Walker, Phys. Rev. Lett. **100**, 031801 (2008); U. Baur and L. H. Orr, Phys. Rev. D **76**, 094012 (2007); **77**, 114001 (2008); Y. Bai and Z. Han, J. High Energy Phys. 04 (2009) 056.

[40] J. Thaler and L. T. Wang, J. High Energy Phys. 07 (2008) 092.

[41] D. E. Kaplan, K. Rehermann, M. D. Schwartz, and B. Tweedie, Phys. Rev. Lett. **101**, 142001 (2008); L. G. Almeida, S. J. Lee, G. Perez, G. Sterman, I. Sung, and J. Virzi, Phys. Rev. D **79**, 074017 (2009); L. G. Almeida, S. J. Lee, G. Perez, I. Sung, and J. Virzi, Phys. Rev. D **79**, 074012 (2009).

[42] A. Pukhov *et al.*, Report No. INP MSU 98-41/542; arXiv: hep-ph/9908288; A. Pukhov, arXiv:hep-ph/0412191.

[43] J. Pumplin, D. R. Stump, J. Huston, H. L. Lai, P. Nadolsky, and W. K. Tung, J. High Energy Phys. 07 (2002) 012.

[44] L. March, E. Ros, and M. Vos, Les Houches BSM Working Group, Twin Higgs Discussion Session, 2007.

[45] T. Sjostrand, S. Mrenna, and P. Skands, J. High Energy Phys. 05 (2006) 026.

[46] D. Benchekroun, C. Driouichi, A. Hoummada, Report No. SN-ATLAS-2001-001 and No. ATL-COM-PHYS-2000-020, EPJ Direct 3, 1 (2001); W. Skiba and D. Tucker-Smith, Phys. Rev. D **75**, 115010 (2007); B. Holdom, J. High Energy Phys. 03 (2007) 063; 08 (2007) 069; M. Strassler, Phenomenology Symposium-Pheno 07, University of Wisconsin, Madison, 2007, pp. 7–9; Gustaaf Brooijmans, Workshop on Possible Parity Restoration at High Energy, Beijing (China), 2007, pp. 11–12; M. H. Seymour, Z. Phys. C **62**, 127 (1994); J. M. Butterworth, B. E. Cox, and J. R. Forshaw, Phys. Rev. D **65**, 096014 (2002); J. M. Butterworth, J. R. Ellis, and A. R. Raklev, J. High Energy Phys. 05 (2007) 033; J. M. Butterworth, A. R. Davison, M. Rubin, and G. P. Salam, Phys. Rev. Lett. **100**, 242001 (2008); AIP Conf. Proc. **1078**, 189 (2009).

[47] C. T. Hill and E. H. Simmons, Phys. Rep. **381**, 235 (2003); **390**, 553(E) (2004).

[48] A. Belyaev, R. Foadi, M. T. Frandsen, M. Jarvinen, F. Sannino, and A. Pukhov, Phys. Rev. D **79**, 035006 (2009); A. R. Zerwekh, Eur. Phys. J. C **46**, 791 (2006).

[49] D. D. Dietrich, F. Sannino, and K. Tuominen, Phys. Rev. D **72**, 055001 (2005).

[50] G. F. Giudice, C. Grojean, A. Pomarol, and R. Rattazzi, J. High Energy Phys. 06 (2007) 045.

[51] M. Perelstein, M. E. Peskin, and A. Pierce, Phys. Rev. D **69**, 075002 (2004); T. Han, H. E. Logan, and L. T. Wang, J. High Energy Phys. 01 (2006) 099; R. Rattazzi, Proc. Sci., LAT2006 (2006) 399 [arXiv:hep-ph/0607058].